

1 A Review of Adjoint Methods for Computing Derivatives Used in Wave Field Inversion

2 William Menke

3 Lamont-Doherty Earth Observatory, Palisades NY

4 MENKE@LDEO.COLUMBIA.EDU

5 July 2016

6

7 Abstract. The wave field imaging techniques that have so revolutionized seismic tomography are
8 predicated on our ability to efficiently compute the derivative of error with respect to a model
9 parameter describing Earth structure. The error quantifies the quality of fit between the observed
10 and predicted data, which can be either the wave field itself (“waveform inversion”) or some
11 quantity derived from it (e.g. finite frequency travel times). Computation of the derivatives is an
12 essential part of the inversion process and usually the most computationally-intensive part of it.
13 Adjoint Methods use a mathematical manipulation drawn from the theory of linear operators to
14 reorganize the calculation, substantially improving its efficiency. We review Adjoint Methods
15 and present simplified derivations of its essential formulas. The concept of the adjoint field is
16 developed, using two complementary techniques: a direct method based on substitution and an
17 implicit one based on Lagrange multipliers. We then show how the introduction of the adjoint
18 field changes the scaling of the derivative calculation, from one proportional to the number of
19 model parameters (which can be very large) to one proportional to the number of receivers
20 (which is typically more modest in size). We derive derivative formula for four types of data: the
21 wave field itself, finite frequency travel times, wave field power, and the cross-convolution
22 measure. In each case, we first develop the general formula and then apply it to the special case
23 of a weakly-heterogeneous medium with a constant background structure.

24
25
26
27
28
29
30
31
32
33
34
35
36
37
38
39
40
41
42
43
44
45
46

1. Introduction

Wave field inversion is the process of inferring Earth structure and/or source parameters from measurements of the seismic wave field. Structural parameters include material properties such as density, compressional velocity and shear velocity and the positions of interfaces. Source parameters include the time histories and spatial patterns of forces and the seismic moment density associated with faulting. The measurements (data) might be the displacement of the wave field, or any of several quantities derived from it, such as finite-frequency travel times Marquering et al. [1999] and cross-convolution measures [Menke and Levin, 2003].

Wave field inversion has been developed by many researchers over the last fifty years and has many different implementations. Most variants employ the principle that the best estimate of the parameters is the one that matches the data to its theoretical prediction. Wave field inversion becomes a nonlinear optimization problem when the misfit between theory and observation is quantified by a formally-defined error (such as the least squares error) and a wide range of well-understood techniques are available to solve it. Among these are iterative methods, which start with an initial estimate of the model, which only poorly fits the data, and successively perturb it to achieve a better fit. Two types of iterative methods are in common use: Newton's method [e.g. Deuffhard, 2004] and the Gradient-Descent method [e.g. Snyman, 2005]. The former method requires the derivative G_{ij} of the predicted data d_i with respect to a model parameter m_j , and the latter requires the derivative g_j of the error with respect to a model parameter:

$$G_{ij} = \frac{\partial d_i}{\partial m_j} \quad \text{and} \quad g_j = \frac{\partial E}{\partial m_j}$$

(1.1 a,b)

47

48

49 Most of the work of wave field inversion (and the cleverness needed to avoid that work) is
50 expended during the computation of these derivatives. These derivatives are often referred to as
51 *sensitivity kernels*, because they quantify how sensitive the predicted data and error are to small
52 changes in the model.

53

54 Like most inversion methods, wave field inversion is predicated on the ability to solve the
55 forward problem; that is, to simulate (predict) the seismic wave field in an arbitrary
56 heterogeneous medium and with a realistic source. Wave field simulation only became practical
57 when the efficiency of computation increased to the point where a complete calculation could be
58 completed in a few hours. Wave field inversion requires many such simulations; the trick is to
59 reduce the number to a manageable level.

60

61 A simplistic analysis based on the finite difference approximation indicates that the time needed
62 to compute a full set of partial derivatives might scale with the number of model parameters M in
63 the Earth model. For example, $M + 1$ simulations are need to compute all M elements of g_j :

64

$$g_j = \frac{\partial E}{\partial m_j} \approx \frac{E(m_j + \Delta m) - E(m_j)}{\Delta m} \quad \text{with } j = 1, \dots, M$$

65

(1.2)

66

67 Wave field inversion currently would be impractical if this was the most efficient possible
68 scaling, because the thousands of parameters needed for realistic Earth models would then imply
69 the need for computing an equal number of wave field simulations (whereas, computing even a
70 few is computationally challenging). Wave field inversion would be limited to a few simplistic
71 cases where the simulation can be computed analytically (such as in homogeneous media
72 [Devaney, 1981]) or where Earth models can be described by just a few parameters (such as
73 layered models [Mellman 1980]).

74

75 Adjoint Methods significantly improved the efficiency of the calculation of derivatives, because
76 they allow the computation to be reorganized so as to scale with the number K of receivers, as
77 contrasted to the number M of model parameters. In a typical seismic imaging problem, $K \ll M$.

78 Adjoint Methods came to seismology via atmospheric science, where they are used to facilitate
79 *data assimilation* - the tuning of the forcing of global circulation models to better match
80 observations [Hall et al., 1982; Hall and Cacuci, 1983; Talagrand and Courtier, 1987]. Early
81 work on seismic wave field sensitivity kernels by Marquering et al. [1998], Marquering et al.
82 [1999], Dahlen et al. [2000] and Hung et al [2000] did not explicitly utilize Adjoint Methods
83 (though some of their mathematical manipulations are arguably similar to them). Adjoint
84 techniques were first introduced into wave field inversion by Tromp et al. [2005], who cite
85 Talagrand and Courtier's [1987] paper as an inspiration. Subsequent work by Zhao et al. [2005],
86 Van der Hilst and De Hoop [2005], Long et al. [2008], Taillandier et al. [2009], Chen et al.
87 [2010], Xu et al. [2012] have developed and extended Adjoint Method. Early applications wave
88 field imaging applied to seismology include Montelli et al.'s [2006] study of mantle plumes,
89 Chen et al.'s [2007] study of the crust beneath southern California, Chauhan et al.'s [2009] study

90 of the Sumatra subduction zones, and Zhu et al. [2012] study of the European continental
91 mantle,.

92 We provide a review here of the underlying principles of the Adjoint Method.

93 Section 2 is devoted to a review of the key concepts of functional analysis and seismic inversion,
94 using mathematical notation that balances compactness with familiarity. Our review of
95 functional analysis includes linear operators and their adjoints and the attributes that make them
96 useful to wave field inversion. The most important relationships are derived and intuitive
97 justifications are provided for most of the rest. Adjoint of selected linear operators are derived
98 in Appendix A.1. A simple example is used to illustrate the potential of Adjoint Methods to
99 improve the efficiency of seismic inversion problems. Our review of inversion includes a
100 discussion of model parameterizations, distinguishes Fréchet derivatives from ordinary partial
101 derivatives, and identifies the cases where their respective use is appropriate. Finally, the role of
102 the Born in calculating perturbations to the wave field is introduced and two complementary
103 derivations are provided.

104 Section 3 reviews the application of the Adjoint Method of *waveform inversion*, that is, special
105 case where the data are the displacement time series, itself, as contrasted to some quantity
106 derived from it (such as a finite-frequency travel time). The least squares error is defined and
107 formulas for the partial derivative of waveform and error with respect to a model parameter and
108 their corresponding Fréchet derivative are derived. The concept of an adjoint field is developed.
109 A direct method is used in the derivations, but the use of an implicit method based on Lagrange
110 multipliers is explored in Appendix A.2. Section 4 applies the results of Section 3 to the simple
111 case of a scalar wave field in a weakly heterogeneous medium with a homogeneous background

112 slowness. The spatial patterns of the partial derivatives are illustrated and its relationship to the
113 seismic migration method is developed.

114

115 Section 5 reviews the application of Adjoint Method to finite frequency travel times. Finite
116 frequency travel time is defined and a perturbation technique is used to derive its partial
117 derivative with respect to a model parameter. An Adjoint Method is then used to derive
118 formulas for the partial derivative of error with respect to a model parameter. Section 6 the
119 results of Section 5 are applied to the scalar wave field case. The spatial patterns of the partial
120 derivative of error are illustrated and their interpretation as a banana-doughnut kernel is
121 developed.

122

123 Section 7 applies the Adjoint Method to the cross-convolution measure, an error-like quantity
124 that is used in receiver function and shear wave splitting imaging, because it is relatively
125 insensitive to the poorly-known source time function of the teleseismic wave field. Formulas for
126 the partial derivatives are developed. Section 8 applies the results of Section 6 to the simple case
127 of an elastic wave field in a weakly heterogeneous medium with homogeneous background
128 slowness. The spatial patterns of the partial derivatives are illustrated and their connection to the
129 issue of model resolution is developed.

130

131 2. Review of Concepts

132

133 2.1. Linear Operators. The word *adjoint* comes from the mathematical theory of linear operators
134 [e.g., Reed and Simon, 1981]. Linear operators, denoted by \mathcal{L} 's, include multiplication by

135 functions, derivatives, integrals and other operations that obey the rule $\mathcal{L}(c_1 f_1 + c_2 f_2) =$
 136 $c_1 \mathcal{L} f_1 + c_2 \mathcal{L} f_2$ (where the c 's are constants and the f 's are functions).
 137
 138 Linear operators act on functions of position and time and are themselves functions of position
 139 and time. Often, we will need to refer to several sets of position and time (e.g. of an observation,
 140 of a source) and so adopt the practice of distinguishing them with subscripts; that is, (\mathbf{x}_A, t_A) and
 141 (\mathbf{x}_B, t_B) . Furthermore, we simplify expressions by abbreviating the functional dependence with a
 142 subscript; that is, $f_A \equiv f(\mathbf{x}_A, t_A)$, $G_{A,B} \equiv G(\mathbf{x}_A, t_A, \mathbf{x}_B, t_B)$, etc.

143
 144 The exemplary expression $f_A = \mathcal{L}_A u_A$ can be interpreted as generating a function f_A from a
 145 function u_A through the action of a linear operator \mathcal{L}_A . It is analogous to the linear algebraic
 146 equation $\mathbf{f} = \mathbf{L}\mathbf{u}$, where \mathbf{u} and \mathbf{f} are time series (vectors) of length M and where \mathbf{L} is a $M \times M$
 147 matrix. The equation $f_A = \mathcal{L}_A u_A$ can be thought of as the limiting case of $\mathbf{f} = \mathbf{L}\mathbf{u}$ when $M \rightarrow \infty$
 148 and the time series become functions. Linear operators are important in seismology because the
 149 wave equation and its solution in terms of Green functions involve linear operators. This
 150 mathematical structure is exemplified by the scalar wave equation for an isotropic homogeneous
 151 material (which has one material parameter, the constant slowness s):

$$\mathcal{L}_A u_A \equiv \left(s^2 \frac{\partial^2}{\partial t_A^2} - \nabla_A^2 \right) u_A = f_A \tag{2.1a}$$

$$u_A = \mathcal{L}_A^{-1} f_A \equiv \int_{t_B} \iiint_{\mathbf{x}_B} F_{A,B} f_B d^3 \mathbf{x}_B dt_B$$

154 (2.1b)

$$\text{with } F_{A,B} \equiv \frac{\delta(t_A - t_B - T_{AB})}{4\pi R_{AB}} \quad \text{with } R_{AB} \equiv |\mathbf{x}_A - \mathbf{x}_B| \quad \text{and } T_{AB} \equiv sR_{AB}$$

155 (2.1c)

156 Here, $F_{A,B}$ is the Green function for an observer at (\mathbf{x}_A, t_A) and an impulsive point source at
157 (\mathbf{x}_B, t_B) and the Dirac impulse function is denoted by $\delta(\cdot)$. The Green function integral is the
158 inverse operator \mathcal{L}_A^{-1} of \mathcal{L}_A (in the sense that \mathcal{L}_A generates f_A from u_A , whereas \mathcal{L}_A^{-1} generates
159 u_A from f_A).

160
161 A linear operator may need to include one or more boundary conditions in order to be fully
162 defined and to possess an inverse. For instance, the simple first derivative equation $f_A =$
163 $\mathcal{L}_A u_A = du_A/dt_A$ needs to be supplemented by the initial condition $u_A(t_A = 0) = 0$ in order for
164 its inverse to be the integral $u_A = \mathcal{L}_A^{-1} f_A = \int_0^{t_A} f_B dt_B$.

165
166 The generalization to the three-component particle displacement field $\mathbf{u} = [u_x, u_y, u_z]^T$ that is
167 commonly used in seismology is algebraically complicated but straightforward. The equations
168 of motion combine Newton's law, $\rho d\dot{u}_i/dt - \sigma_{ij,j} = f_i$ (where ρ is density and σ is stress)
169 with Hooke's Law $\sigma_{ij} = c_{ijpq} u_{p,q}$ (where c_{ijpq} is the elastic tensor) to yield the second-order
170 matrix differential equation $\mathcal{L}_A \mathbf{u}_A = \mathbf{f}_A$. In the isotropic case with Lamé parameters λ and μ , the
171 operator \mathcal{L}_A is 3×3 :

172

$$\mathcal{L}_A \mathbf{u} = (\mathcal{L}_A^{(1)} + \mathcal{L}_A^{(2)}) \mathbf{u}_A = \mathbf{f}_A = \begin{bmatrix} f_x \\ f_y \\ f_z \end{bmatrix}_A$$

173

$$\mathcal{L}_A^{(1)} = \begin{bmatrix} \rho \frac{\partial^2}{\partial t^2} - (\lambda + 2\mu) \frac{\partial^2}{\partial x^2} - \mu \frac{\partial^2}{\partial y^2} - \mu \frac{\partial^2}{\partial z^2} & -(\lambda + \mu) \frac{\partial^2}{\partial x \partial y} & -(\lambda + \mu) \frac{\partial^2}{\partial x \partial z} \\ -(\lambda + \mu) \frac{\partial^2}{\partial x \partial y} & \rho \frac{\partial^2}{\partial t^2} - \mu \frac{\partial^2}{\partial x^2} - (\lambda + 2\mu) \frac{\partial^2}{\partial y^2} - \mu \frac{\partial^2}{\partial z^2} & -(\lambda + \mu) \frac{\partial^2}{\partial y \partial z} \\ -(\lambda + \mu) \frac{\partial^2}{\partial x \partial z} & -(\lambda + \mu) \frac{\partial^2}{\partial y \partial z} & \rho \frac{\partial^2}{\partial t^2} - \mu \frac{\partial^2}{\partial x^2} - \mu \frac{\partial^2}{\partial y^2} - (\lambda + 2\mu) \frac{\partial^2}{\partial z^2} \end{bmatrix}$$

174

$$\mathcal{L}_A^{(2)} = - \begin{bmatrix} \frac{\partial(\lambda + 2\mu)}{\partial x} \frac{\partial}{\partial x} + \frac{\partial\mu}{\partial y} \frac{\partial}{\partial y} + \frac{\partial\mu}{\partial z} \frac{\partial}{\partial z} & \frac{\partial\lambda}{\partial x} \frac{\partial}{\partial y} + \frac{\partial\mu}{\partial y} \frac{\partial}{\partial x} & \frac{\partial\lambda}{\partial x} \frac{\partial}{\partial z} + \frac{\partial\mu}{\partial z} \frac{\partial}{\partial x} \\ \frac{\partial\lambda}{\partial y} \frac{\partial}{\partial x} + \frac{\partial\mu}{\partial x} \frac{\partial}{\partial y} & \frac{\partial\mu}{\partial x} \frac{\partial}{\partial x} + \frac{\partial(\lambda + 2\mu)}{\partial y} \frac{\partial}{\partial y} + \frac{\partial\mu}{\partial z} \frac{\partial}{\partial z} & \frac{\partial\lambda}{\partial y} \frac{\partial}{\partial z} + \frac{\partial\mu}{\partial z} \frac{\partial}{\partial y} \\ \frac{\partial\lambda}{\partial z} \frac{\partial}{\partial x} + \frac{\partial\mu}{\partial x} \frac{\partial}{\partial z} & \frac{\partial\lambda}{\partial z} \frac{\partial}{\partial y} + \frac{\partial\mu}{\partial y} \frac{\partial}{\partial z} & \frac{\partial\mu}{\partial x} \frac{\partial}{\partial x} + \frac{\partial\mu}{\partial y} \frac{\partial}{\partial y} + \frac{\partial(\lambda + 2\mu)}{\partial z} \frac{\partial}{\partial z} \end{bmatrix}$$

175

(2.2)

176

177 Here, we have written the operator \mathcal{L} as the sum of a term $\mathcal{L}^{(1)}$ that does not contain derivatives
 178 of the material parameters and a term $\mathcal{L}^{(2)}$ that does. We have also suppressed the subscript A on
 179 the derivatives to improve readability of the matrices.

180

181 Some authors use two coupled first-order equations, in particle velocity and strain, rather than
 182 the single second-order equation, above. The combined matrix equation is larger but
 183 algebraically simpler and more amenable to numerical integration.

184

185 2.2. The Inner Product. Central to the theory of linear operators is the concept of the inner
 186 product, which computes a number q from an arbitrary pair of functions u_A and v_A :

187

$$q = \int_{t_A} \iiint_{\mathbf{x}_A} u_A v_A d^3 \mathbf{x}_A dt_A \equiv \langle u_A, v_A \rangle_A$$

188 (2.3)

189

190 The angle brackets provide a compact way of writing the inner product. The subscript A in $\langle \cdot, \cdot \rangle_A$

191 indicates that the integration is over (\mathbf{x}_A, t_A) . The location of the comma is significant only when

192 its arguments are more complicated than simple functions. For instance, $\langle \mathcal{L}_A u_A, v_A \rangle_A$ implies that

193 the linear operator \mathcal{L}_A is applied to u_A but not v_A . The inner product of functions u_A and v_A is

194 analogous to the dot product $s = \sum_i u_i v_i = \mathbf{u}^T \mathbf{v}$ of vectors \mathbf{u} and \mathbf{v} . Furthermore, just as

195 $\ell^2 = \mathbf{u}^T \mathbf{u}$ is the squared length of the vector \mathbf{u} and $d^2 = (\mathbf{u} - \mathbf{v})^T (\mathbf{u} - \mathbf{v})$ is the squared

196 distance between vectors \mathbf{u} and \mathbf{v} , so $\ell^2 = \langle u_A, u_A \rangle_A$ can be thought of as the squared length of

197 the function u_A and $d^2 = \langle u_A - v_A, u_A - v_A \rangle_A$ can be thought of the distance between the two

198 functions u_A and v_A . Thus, like the dot product, the inner product is very useful in quantifying

199 sizes and distances. An important inner product in seismology is the waveform error $E_T =$

200 $\langle u_A^{obs} - u_A, u_A^{obs} - u_A \rangle_A$, which defines the total error (misfit) between and observed and

201 predicted wave fields.

202

203 In the case of a vector field, the inner product is the integral of the dot product of the fields:

204

$$q = \int_{t_A} \iiint_{\mathbf{x}_A} [\mathbf{u}_A]^T \mathbf{v}_A d^3 \mathbf{x}_A dt_A \equiv \langle \mathbf{u}, \mathbf{v} \rangle_A$$

205

206 (2.4)

207

208 2.3. The Adjoint of a Linear Operator. One or both of the arguments of an inner product can
 209 involve a linear operator \mathcal{L}_A - for example, $\langle \mathcal{L}_A u_A, v_A \rangle_A$. This situation is analogous to a dot
 210 product containing a matrix \mathbf{L} - for example $(\mathbf{L}\mathbf{u})^T(\mathbf{v})$. In the latter case, the transposition
 211 operator can be used to “move” the matrix from one part of the dot product to the other, in the
 212 sense that $(\mathbf{L}\mathbf{u})^T(\mathbf{v}) = (\mathbf{u})^T(\mathbf{L}^T\mathbf{v})$. The *adjoint operator*, which is denoted with the dagger
 213 symbol \dagger , moves the linear operator from one side of the inner product to the other in a
 214 completely analogous way: $\langle \mathcal{L}_A u_A, v_A \rangle_A = \langle u_A, \mathcal{L}_A^\dagger v_A \rangle_A$. Just as \mathbf{L}^T is a different matrix from \mathbf{L} ,
 215 but constructed from it in a known way (that is, by swapping rows and columns), so the operator
 216 \mathcal{L}_A^\dagger is different from the operator \mathcal{L}_A but constructed from it in a known way (though in a way
 217 more complicated than for a matrix). Thus, far from being mysterious, the adjoint is just a
 218 $M \rightarrow \infty$ limiting case of a matrix transpose. Adjoint operators obey almost all of the same algebraic rules
 219 as do transposes, including:

$$\mathcal{L}_A^{\dagger\dagger} = \mathcal{L}_A \quad \text{and} \quad (\mathcal{L}_A^\dagger)^{-1} = (\mathcal{L}_A^{-1})^\dagger \quad \text{and} \quad (\mathcal{L}_A^{(1)} \mathcal{L}_A^{(2)})^\dagger = (\mathcal{L}_A^{(2)})^\dagger (\mathcal{L}_A^{(1)})^\dagger$$

(2.5)

223 Just as a matrix that obeys $\mathbf{L}^T = \mathbf{L}$ or $\mathbf{L}^T = -\mathbf{L}$ is respectively called symmetric or anti-
 224 symmetric, so an operator that obeys $\mathcal{L}_A^\dagger = \mathcal{L}_A$ or $\mathcal{L}_A^\dagger = -\mathcal{L}_A$ is respectively called *self-adjoint* or
 225 *anti-self-adjoint*. A few simple cases are (see Appendix A.1):

$$\mathcal{L}u \qquad \qquad \qquad \mathcal{L}^\dagger u \qquad \qquad \qquad 2.6a$$

$$c(\mathbf{x}, t) u \qquad \qquad \qquad \text{self-adjoint} \qquad \qquad \qquad 2.6b$$

du/dt and du/dx	anti-self-adjoint	2.6c
d^2u/dt^2 and d^2u/dx^2	self-adjoint	2.6d
$\begin{bmatrix} \mathcal{L}_{11} & \mathcal{L}_{12} \\ \mathcal{L}_{21} & \mathcal{L}_{22} \end{bmatrix} \begin{bmatrix} u_1 \\ u_2 \end{bmatrix}$	$\begin{bmatrix} \mathcal{L}_{11}^\dagger & \mathcal{L}_{12}^\dagger \\ \mathcal{L}_{21}^\dagger & \mathcal{L}_{22}^\dagger \end{bmatrix}^T \begin{bmatrix} u_1 \\ u_2 \end{bmatrix}$	2.6e
$a(t) * u$	$a(t) \star u$	2.6f
$\mathcal{L}u$ of elastic wave equation	self-adjoint	2.6g
$\langle \mathcal{F}_{B,A}, u_A \rangle_A$	$\langle \mathcal{F}_{A,B}^\dagger, u_A \rangle_A$	2.6g

227

228 Here * signifies convolution and \star signifies cross-correlation. Taking the adjoint of a first
 229 derivative reverse the sense of direction of the independent variable, since $-d/dt = d/d(-t)$
 230 and $-d/dx = d/d(-x)$ This effect is more important for the time than for space, because the
 231 time boundary condition is usually asymmetric (the past is quiescent but the future is not), while
 232 the space boundary condition is usually symmetric (the field approaches zero as $x \rightarrow \pm\infty$).
 233 Consequently, manipulations of equations using adjoints often lead to behaviors that are
 234 “backward in time” (see Appendix A.1).

235

236 2.4. Applications of Adjuncts. Two factors combine to make Adjoint Methods especially useful
 237 in seismology. First, observations often involve a wave field u that obeys a differential equation
 238 $\mathcal{L}_A u_A = f_A$ (where f_A is a source term), so a linear operator \mathcal{L}_A is associated with the problem.
 239 Second, the formulas that link the field u to observations and to observational error involve inner
 240 products.

241

242 To see why this combination of factors might be useful, consider the case where a set of N
 243 observations d_i^{obs} are related to the field u by the inner product [see Menke, Section 11.11,
 244 2012]; that is, the predicted data is:

$$d_i = \langle h_{Ai}, u_A \rangle_A \tag{2.7}$$

245
 246
 247
 248 Here, $h_{Ai} \equiv h_i(\mathbf{x}_A, t_A)$ are known functions and u_A is the wave field. Now suppose that we want
 249 to “tune” the source so that the observations are matched (meaning we inverting for the source
 250 f_A). A perturbation δf_A in the source causes a perturbation δu_A in the field which, in turn, causes
 251 a perturbation δd_i in the data. Because of the linearity of the system:

$$\mathcal{L} \delta u_A = \delta f_A \quad \text{and} \quad \delta d_i = \langle h_{Ai}, \delta u_A \rangle_A \tag{2.8}$$

252
 253
 254
 255 Writing the solution of the differential equation as $\delta u_A = \mathcal{L}^{-1} \delta f_A$ and inserting it into the inner
 256 product yields:

$$\delta d_i = \langle h_{Ai}, \mathcal{L}^{-1} \delta f_A \rangle_A = \langle h_{Ai}, \delta u_A \rangle_A \quad \text{with} \quad \mathcal{L} \delta u_A = \delta f_A \tag{2.9}$$

257
 258
 259 This equation reads: to determine the perturbation δd_i in the data, solve the wave equation with a
 260 source perturbation δf_A to determine the field perturbation δu_A and then take the inner product
 261 of δu_A with the function h_{Ai} . The differential equation must be solved for every source

262 perturbation δf_A that is considered (let's suppose that there are M of them), but once these
263 solutions are determined, they can be applied to any number of data. Now, suppose that we
264 manipulate the inner product:

$$\delta d_i = \langle \mathcal{L}^{+-1} h_{Ai}, \delta f_A \rangle_A \equiv \langle \lambda_{Ai}, \delta f_A \rangle_A \quad \text{with} \quad \mathcal{L}^+ \lambda_{Ai} = h_{Ai} \quad (2.10)$$

267
268 Here we have introduced the *adjoint field* $\lambda_{Ai} \equiv \lambda_i(\mathbf{x}_A, t_A)$ as an abbreviation for $\mathcal{L}^{+-1} h_{Ai}$. This
269 equation reads: to determine the perturbation δd_i in the data, solve the adjoint differential
270 equation with source term h_{Ai} to determine the adjoint field λ_{Ai} and then take the inner product
271 of λ_{Ai} with the source perturbation δf_A . The adjoint differential equation needs be solved N
272 times (once for each datum), but once these solutions are determined, they can be applied to any
273 number of source perturbations.

274
275 As an aside, we mention that the adjoint field plays the role of a *data kernel* G_{Ai} linking
276 perturbations in data to perturbations in unknowns, that is $\delta d_i = \langle G_{Ai}, \delta f_A \rangle_A$ with $G_{Ai} \equiv \lambda_{Ai}$.

277
278 In many practical problems, $M \gg N$, so the adjoint formulation is preferred. The advantage is
279 one of efficiency, only; both approaches lead to same solution. However, the value of efficiency
280 must not be underrated, for many problems in seismology become tractable *only* because of
281 Adjoint methods.

282

283 In seismology, this procedure can be used to determine the earthquake source, as quantified by
 284 its moment tensor density, from observed seismic waves [Kim et al., 2011]. The function h_{Ai} in
 285 Equation (2.7) is then the Dirac delta function $\delta(\mathbf{x}_R - \mathbf{x}_A)\delta(t_R - t_A)$; that is, the predicted data
 286 d_i is the field u_i observed at time t_R by a receiver at \mathbf{x}_R .

287

288 2.5. The Fréchet derivative. The equation $\delta d_i = \langle G_{Ai}, \delta f_A \rangle_A$ is very similar in structure to the
 289 first order perturbation rule for a set of analogous vector quantities $\Delta \mathbf{d}$ and $\Delta \mathbf{f}$:

290

$$\Delta d_i = (\mathbf{G}^{(i)})^T \Delta \mathbf{f} = \sum_j \frac{\partial d_i}{\partial f_j} \Delta f_j \quad \text{with} \quad \frac{\partial d_i}{\partial f_j} \equiv G_{ij}$$

291

(2.11)

292

293 The only differences are that the vector $\Delta \mathbf{f}$ has been replaced by the function δf_A and the
 294 summation has been replaced by integrals. Consequently, the rule $\delta d_i = \langle G_{Ai}, \delta f_A \rangle_A$ can be
 295 thought of defining a kind of derivative:

296

$$\delta d_i = \langle G_{Ai}, \delta f_A \rangle_A \equiv \int_{t_A} \iiint_{\mathbf{x}_A} \frac{\delta d_i}{\delta f_A} \delta f_A d^3 \mathbf{x}_A dt_A \equiv \left\langle \frac{\delta d_i}{\delta f}, \delta f_A \right\rangle_A \quad \text{with} \quad \frac{\delta d_i}{\delta f_A} \equiv G_{Ai}$$

297

(2.12)

298

299 This so-called *Fréchet derivative* $\delta d_i / \delta f_A$ is distinguished from a partial derivative by the use of
 300 δ 's in place of ∂ 's. Partial derivative Fréchet derivatives find many uses, especially because they
 301 obey the *chain rule*:

302

$$\frac{\delta d_i}{\delta f_A} = \left\langle \frac{\delta d_i}{\delta u_B}, \frac{\delta u_B}{\delta f_A} \right\rangle_B$$

303 (2.13)

304

305 Here u_B is an arbitrary function of space and time. The manipulation of expressions into a form
 306 that identifies a Fréchet derivative (as in the case above) is another important application of
 307 Adjoint methods.

308

309 2.6. Model Parameterization. In the case discussed above, the source perturbation δf_A is treated
 310 as the unknown. Far more common in seismology is the case where the material parameters that
 311 appear in \mathcal{L}_A , such as elastic constants and density, are the unknowns. An important question is
 312 whether these parameters should be described by a spatially (and possibly temporally) varying
 313 function, say $m_A \equiv m(\mathbf{x}, t)$, (as was done previously for the source) or by a set of discrete
 314 parameters $m_i, i = 1 \dots M$ that multiply a set of prescribed spatial-temporal patterns. (say
 315 $p_A^{(i)} = p_i(\mathbf{x}_A, t_A)$):

316

$$\delta m(\mathbf{x}_A, t_A) = \sum_{i=1}^M m_i p^{(i)}(\mathbf{x}_A, t_A) \quad \text{or} \quad \delta m_A = \sum_{i=1}^M m_i p_A^{(i)}$$

317 (2.14)

318

319 The issue is where in the solution process the transition should be made from a continuous view
 320 of the world, which is realistic but unknowable, to a discrete view, which is approximate but
 321 computable. The first approach starts with the derivation of Fréchet derivatives and converts
 322 them to partial derivatives only at last resort. The second approach uses only partial derivatives

323 throughout. We review both approaches here, because both are used in the literature.

324

325 2.7. The Born Approximation. The differential equation $\mathcal{L}_A(m) u_A = f_A$ is not, in general, linear
326 in a material parameter m , so only an approximate equation can be derived that links a

327 perturbation in the material parameter to a perturbation in the field. This is in contrast to the case

328 of the unknown source, in which the equation $\mathcal{L}_A \delta u_A = \delta f_A$ is exact. Here we examine the case

329 for a single discrete parameter m_1 (for which we subsequently drop the subscript). The result

330 can be generalized to multiple discrete parameters m_i merely by adding a substituting m_i for m .

331 The generalization to the continuous case is somewhat more complicated and will be derived

332 later. We compare two different approaches to deriving this equation, which, as we will discover,

333 yield the same result.

334

335 The first approach starts with the equation $u_A = \mathcal{L}_A^{-1} f_A$ and differentiates it with respect to m

336 around a point m^0

337

$$\begin{aligned} \frac{\partial u_A}{\partial m} \Big|_{m^0} &= \frac{\partial (\mathcal{L}_A^{-1} f_A)}{\partial m} \Big|_{m^0} = \frac{\partial}{\partial m} \mathcal{L}_A^{-1} \Big|_{m^0} f_A = \\ &-\mathcal{L}_A^{-1} \Big|_{m^0} \frac{\partial \mathcal{L}_A}{\partial m} \Big|_{m^0} \mathcal{L}_A^{-1} \Big|_{m^0} f_A = -\mathcal{L}_A^{-1} \Big|_{m^0} \frac{\partial \mathcal{L}_A}{\partial m} \Big|_{m^0} u_A^0 \equiv G_A \end{aligned}$$

338

(2.15)

339

340 Note that f_A is not a function of m , so that $\partial f_A / \partial m = 0$, that $u_A^0 = \mathcal{L}_A^{-1} \Big|_{m^0} f_A$ is the solution to

341 the *unperturbed* equation $\mathcal{L}_A \Big|_{m^0} u_A^0 = f_A$, G is the data kernel (the partial derivative of the field

342 with respect to a model parameter), and the derivation uses the derivative rule (Appendix A.2):

343

$$\frac{\partial}{\partial m} \mathcal{L}_A^{-1} = -\mathcal{L}_A^{-1} \frac{\partial \mathcal{L}_A}{\partial m} \mathcal{L}_A^{-1}$$

344

(2.16)

345

346 The second approach starts with the wave equation $\mathcal{L}_A(m) u_A = f_A$, represents the field $u_A =$ 347 $u_A^0 + \Delta u_A$ as the sum of an unperturbed part u_A^0 and a perturbation Δu_A and expands the operator348 $\mathcal{L}(m)$ around the point m^0 , discarding terms higher than first-order:

349

$$\mathcal{L}_A(m) = \mathcal{L}_A|_{m^0} + \left. \frac{\partial \mathcal{L}_A}{\partial m} \right|_{m^0} \Delta m$$

350

(2.17)

351

352 Inserting these representations into the wave equation and keeping only first order terms (the

353 *Born approximation*) yields:

354

$$f_A = \left(\mathcal{L}_A|_{m^0} + \left. \frac{\partial \mathcal{L}_A}{\partial m} \right|_{m^0} \Delta m \right) (u_A^0 + \Delta u_A) = \mathcal{L}_A|_{m^0} u_A^0 + \left. \frac{\partial \mathcal{L}_A}{\partial m} \right|_{m^0} u_A^0 \Delta m + \mathcal{L}_A|_{m^0} \Delta u_A$$

355

(2.18)

356

357 Subtracting out the unperturbed equation and rearranging yields:

358

$$\Delta u_A = \left(-\mathcal{L}_A^{-1}|_{m^0} \left. \frac{\partial \mathcal{L}_A}{\partial m} \right|_{m^0} u_A^0 \right) \Delta m \equiv \frac{\partial u_A}{\partial m} \Delta m \equiv G_A \Delta m$$

359

(2.19)

360

361 We can now identify the data kernel $G_A \equiv \partial u_A / \partial m$ as the factor in the parentheses and see that
362 it's the same formula that was derived by the first approach. That these two approaches lead to
363 the same formula is unsurprising, since both are based on first-order approximations of the same
364 equations.

365

366 2.8. An Exemplary Partial Derivative of an Operator. The partial derivative $\partial \mathcal{L}_A / \partial m$ may at first
367 seem mysterious, but an example demonstrates that it is completely straightforward. Consider the
368 special case of a scalar wave equation with slowness $s_A = s_{0A} + \delta s_A$, where the unperturbed
369 slowness s_{0A} and the perturbation δs_A are both spatially-variable functions. We parameterize
370 $\delta s_A = m p_A$, where p_A is prescribed "pattern" function and m is a scalar amplitude parameter.
371 The linear operator in the wave equation is then:

$$\mathcal{L}_A(m) = [s_{0A} + \delta s_A]^2 \frac{\partial^2}{\partial t_A^2} - \nabla_A^2 \approx [s_{0A}^2 + 2s_{0A}m p_A] \frac{\partial^2}{\partial t_A^2} - \nabla_A^2$$

372 (2.20)

373 Taking the partial derivative with respect to m and evaluating it at $m = m^0 = 0$ yields:

$$\left. \frac{\partial \mathcal{L}_A}{\partial m} \right|_0 = 2s_{0A} p_A \frac{\partial^2}{\partial t_A^2}$$

374 (2.21)

375

376 2.9. Relationship between a partial derivative and a Fréchet derivative. Suppose that the model
377 is parameterized as $\delta m_A = p_A \Delta m$ where p_A is a prescribed spatially and temporally varying

378 pattern and Δm is a scalar. Inserting this form of δm into the Fréchet derivative $\delta u_A =$
 379 $\langle \delta u_A / \delta m_B, \delta m_B \rangle_B$ yields:

380

$$\delta u_A = \left\langle \frac{\delta u_A}{\delta m_B}, p_B \right\rangle_B \Delta m = \frac{\partial u_A}{\partial m} \Delta m \quad \text{with} \quad \frac{\partial u_A}{\partial m} \equiv \left\langle \frac{\delta u_B}{\delta m}, p_B \right\rangle_B$$

381

(2.22)

382

383 Evidentially, the partial derivative can be formed by taking the inner product of the Fréchet
 384 derivative with the prescribed pattern. Alternately, suppose that the pattern is temporally- and
 385 spatially localized at B ; that is $\delta m_{A,B} = m \delta(t_A - t_B) \delta(\mathbf{x}_A - \mathbf{x}_B)$ where m is a scalar model
 386 parameter. Furthermore, suppose that this model function leads to the partial derivative is
 387 $\partial u_{A,B} / \partial m$. The effect of many such perturbations, each with its own position \mathbf{x}_B , time t_B , and
 388 amplitude δm_B , is the superposition (integral) of the individual ones:

389

$$(\delta u_A)^{\text{total}} = \left\langle \frac{\partial u_{A,B}}{\partial m}, \delta m_B \right\rangle_B \quad \text{with} \quad \frac{\delta u_A}{\delta m_B} \equiv \frac{\partial u_{A,B}}{\partial m_B}$$

390

(2.23)

391

392 Evidentially, the Fréchet derivative is just the partial derivative for a temporally- and spatially
 393 localized pattern.

394 3. Waveform Tomography

395

396 3.1. Definition of Error. The goal in waveform tomography is to match the predicted field u_A to
 397 the observed field u_A^{obs} , by minimizing the total error $E = \langle e_A, e_A \rangle_A$, where $e_A = u_A^{\text{obs}} - u_A$.

398 This optimization problem can be solved using the Gradient-Descent method, which minimize
 399 E by iteratively perturbs an initial estimate of m . It requires the either the partial derivative
 400 $\partial E / \partial m$ or the Fréchet derivative $\delta E / \delta m$, depending upon whether the model is respectively
 401 represented by discrete parameters or continuous functions.

402 3.2. Partial Derivative of Error. As before, the predicted field u_A is assumed to arise through the
 403 solution of a differential equation $\mathcal{L}_A(m) u_A = f_A$ containing a discrete parameter m . A
 404 perturbation Δm in parameter m causes a perturbation ΔE in the total error E_T :

$$\Delta E = \left. \frac{\partial E}{\partial m} \right|_{m_0} \Delta m \quad \text{where} \quad \frac{\partial E}{\partial m} = 2 \left\langle e_A^0, \left. \frac{\partial e_A}{\partial m} \right|_{m_0} \right\rangle = -2 \left\langle e_A^0, \left. \frac{\partial u_A}{\partial m} \right|_{m_0} \right\rangle = -2 \langle e_A^0, G_A \rangle_A$$

405 (3.1)

406 We simplify the notation used in subsequent equations by dropping explicit dependence on m_0 .

407 Inserting the formula for G_A yields:

$$\frac{\partial E}{\partial m} = -2 \langle e_A, G_A \rangle = 2 \langle e_A^0, \mathcal{L}_A^{-1} \frac{\partial \mathcal{L}_A}{\partial m} u_A^0 \rangle_A = \left\langle 2 \frac{\partial \mathcal{L}_A^\dagger}{\partial m} \mathcal{L}_A^{-1\dagger} e_A^0, u_A^0 \right\rangle_A = \langle h_A, u_A^0 \rangle_A$$

$$\text{with } h_A = 2 \frac{\partial \mathcal{L}_A^\dagger}{\partial m} \lambda_A \quad \text{and} \quad \lambda_A = \mathcal{L}_A^{-1\dagger} e_A^0 \quad \text{or} \quad \mathcal{L}_A^\dagger \lambda_A = e_A^0$$

408 (3.2)

409 As before, we have introduced an adjoint field λ_A . The derivative $\partial E / \partial m$ is constructed as
 410 follows: First, the adjoint field λ_A is determined by solving the adjoint wave equation, which
 411 involves the adjoint operator \mathcal{L}_A^\dagger and has a source term equal to the prediction error e_A^0 . Second,
 412 the operator $2 \partial \mathcal{L}_A^\dagger / \partial m$ is applied to the adjoint field to yield the function h_A . Finally, the inner

413 product of the unperturbed field e_A^0 with the function h is computed. This process is often
 414 referred to as *correlating* h_A and e_A^0 , since it corresponds to their zero-lag cross-correlation.

415 In many practical cases, we will want to consider the error E_R associated with one receiver point
 416 R :

$$E_R = E(\mathbf{x}_R) = \int [u^{obs}(\mathbf{x}_R, t_R) - u(\mathbf{x}_R, t_R)]^2 dt_R$$

417 (3.3)

418 We now assert that the total error E_T is the superposition of the individual errors E_R , its partial
 419 derivative is the superposition of individual partial derivatives, and the adjoint field λ_A is the
 420 superposition of individual $\lambda_{A,R}$'s:

$$E_T = \int E_R d^3x_R \quad \text{and} \quad \frac{\partial E_T}{\partial m} = \int \frac{\partial E_R}{\partial m} d^3x_R \quad \text{and} \quad \lambda_A = \int \lambda_{A,R} d^3x_R$$

421 (3.4)

422 Inserting this definition of $\lambda_{A,R}$ into the differential equation for λ_A yields:

$$\mathcal{L}_A^\dagger \lambda_A - e_A^0 = 0$$

$$\mathcal{L}_A^\dagger \int \lambda_{A,R} d^3x_R - \int e^0(\mathbf{x}_R, t_A) \delta(\mathbf{x}_A - \mathbf{x}_R) d^3x_R = 0$$

$$\int \{ \mathcal{L}_A^\dagger \lambda_{A,R} - e^0(\mathbf{x}_R, t) \delta(\mathbf{x}_A - \mathbf{x}_R) \} d^3x_R = 0$$

423 (3.5)

424 The presumption that this equation holds irrespective of the volume over which the error is
425 defined implies that the integrand is zero, so:

$$\mathcal{L}_A^\dagger \lambda_{A,R} = e^0(\mathbf{x}_R, t) \delta(\mathbf{x}_A - \mathbf{x}_R)$$

426 (3.6)

427 Thus, each $\lambda_{A,R}$ corresponds to a point source at \mathbf{x}_R with the time function of the error at that
428 point. Similarly, if we define $h_{A,R} \equiv 2[\partial\mathcal{L}_A^\dagger/\partial m] \lambda_{A,R}$, then a procedure analogous to the one
429 above can be used to show that:

$$\frac{\partial E_R}{\partial m} = \langle h_{A,R}, u_A^0 \rangle_A$$

430 (3.7)

431 A typical seismological application might involve $M \approx 10^4$ model parameters but only $K \approx 10^2$
432 observations points. The adjoint formulation allows all 10^4 partial derivatives (one for each
433 model parameter) to be calculated by solving “only” $K + 1$ differential equations, one to
434 calculate the unperturbed field u^0 and the rest to calculate the adjoint fields, of which there is
435 one for each of the K observation points.

436 Physically, the adjoint field can be thought of as the scattered field, back-propagated to
437 heterogeneities from which it *might* have originated. Mathematically, the adjoint field can be
438 interpreted as a Lagrange multiplier associated with the constraint that the field obeys a wave
439 equation at every point in space and time (see Appendix A.3).

440 3.3. Fréchet Derivative of Error. We now present a completely parallel derivation of the Fréchet
 441 derivative of the waveform error with respect to a model function m_A . The scalar field u_A
 442 satisfies partial differential equation:

$$\mathcal{L}_A(m_A) u_A = f_A$$

444 (3.8)

445 We will write both u_A and m_A in terms of background level and a perturbation:

$$u_A = u_A^0 + \delta u_A \quad \text{and} \quad m_A = m_A^0 + \delta m_A$$

446 (3.9)

447 Functions u_A^0 , δu_A , m_A^0 and δm_A all vary with both space and time. However, in most practical
 448 cases m_A and δm_A will be constant in time. The background field u_A^0 satisfies the unperturbed
 449 equation:

$$\mathcal{L}_A(m_A^0) u_A^0 = f_A$$

451 (3.10)

452 The Fréchet derivative for the total error $E_T = \langle e_B, e_B \rangle_B$ with $e_B = u_B^{obs} - u_B$ and $e_B^0 = u_B^{obs} -$
 453 u_B^0 , is derived by considering how a perturbation in the field changes the error:

$$\begin{aligned} \delta E_T &= \langle e_B, e_B \rangle_B - \langle e_B^0, e_B^0 \rangle_B = \langle e_B^0 + \delta e_B, e_B^0 + \delta e_B \rangle_B - \langle e_B^0, e_B^0 \rangle_B \\ &= \langle e_B^0, e_B^0 \rangle_B + 2\langle e_B^0, \delta e_B \rangle_B + \langle \delta e_B, \delta e_B \rangle_B - \langle e_B^0, e_B^0 \rangle_B \end{aligned}$$

$$= \langle 2e_B, \delta e_B \rangle_B - \langle \delta u_B, \delta e_B \rangle_B \approx \langle 2e_B^0, \delta e_B \rangle_B$$

454 (3.11)

455 Note that we have discarded terms of second order in small quantities. Substituting in $\delta e_B =$
 456 $-\delta u_B$ yields:

$$\delta E_T = \langle -2e_B^0, \delta u_B \rangle_B$$

457 (3.12)

458 The next step is to replace δu_B in the above expression with an expression involving δm_B . We
 459 start with the Fréchet derivative of the field, which is defined by:

460

$$\delta u_A = \left\langle \left[\frac{\delta u}{\delta m} \right]_{A,B}, \delta m_B \right\rangle_B \equiv \langle G_{A,B}, \delta m_B \rangle_B \equiv \mathcal{G}_A \delta m_A$$

461 (3.13)

462 Here the inner product with Fréchet derivative $G_{A,B} \equiv [\delta u_A / \delta m_B]$ is understood to be a linear
 463 operator \mathcal{G}_A . Our derivation requires the Fréchet derivative of the operator $\mathcal{L}_A(m)$. It satisfies:

$$\delta \mathcal{L}_A = \left\langle \frac{\delta \mathcal{L}_A}{\delta m_B}, \delta m_B \right\rangle_B$$

464 (3.14)

465 As shown previously, this is just the partial derivative of the operator for a heterogeneity
 466 temporally- and spatially-localized at B . For example, in the case of the scalar wave equation:

$$\mathcal{L}_A(m_A) = \left\{ (m_A^0)^2 \frac{\partial^2}{\partial t_A^2} - \nabla_A^2 \right\} + 2m_A^0 m_B \delta(\mathbf{x}_A - \mathbf{x}_B) \delta(t_A - t_B) \frac{\partial^2}{\partial t_A^2}$$

$$\frac{\delta \mathcal{L}_A}{\delta m_B} = \frac{\partial \mathcal{L}_A}{\partial m_B} = 2m_A^0 \delta(\mathbf{x}_A - \mathbf{x}_B) \delta(t_A - t_B) \frac{\partial^2}{\partial t_A^2}$$

467 (3.15)

468 The Fréchet derivative of the field is then derived by applying the Born approximation to the
 469 differential equation:

$$\mathcal{L}_A(m_A) u_A = f_A$$

$$(\mathcal{L}_A(m_A^0) + \delta \mathcal{L}_A(m_A)) (u_A^0 + \delta u_A) = f_A$$

$$\left(\mathcal{L}_A(m_A^0) + \left\langle \frac{\delta \mathcal{L}_A}{\delta m_B}, \delta m_B \right\rangle_B \right) (u_A^0 + \delta u_A) = f_A$$

$$\mathcal{L}_A(m_A^0) u_A^0 + \mathcal{L}_A(m_A^0) \delta u_A + \left\langle \frac{\delta \mathcal{L}_A}{\delta m_B}, \delta m_B \right\rangle_B u_A^0 \approx f_A$$

470 (3.16)

471 Subtracting out the unperturbed equation and rearranging yields:

$$\delta u_A = \left\langle -\mathcal{L}_A^{-1} \frac{\delta \mathcal{L}_A}{\delta m_B} u_A^0, \delta m_B \right\rangle_B \equiv \langle G_{A,B}, \delta m_B \rangle_B \equiv \mathcal{G}_A \delta m_A$$

$$G_{A,B} = -\mathcal{L}_A^{-1} \frac{\delta \mathcal{L}_A}{\delta m_B} u_A^0$$

472 (3.17)

473 The Fréchet derivative of the total error with respect to the model is obtained by substituting
 474 $\delta u_B = \mathcal{G}_B \delta m_B$ into the general expression for this derivative:

$$\delta E_T = \langle -2e_B^0, \mathcal{G}_B \delta m_B \rangle_B = \langle -2\mathcal{G}_B^\dagger e_B^0, \delta m_B \rangle_B$$

475 (3.18)

476 The Fréchet derivative of the total error is then:

$$\frac{\delta E_T}{\delta m_A} = -2\mathcal{G}_A^\dagger e_A^0 = \langle u_B^0, \mathcal{G}_{B,A}^\dagger e_B^0 \rangle_B = \langle \mathcal{G}_{B,A}^\dagger e_B, u_B^0 \rangle_B$$

477 (3.19)

478 Substituting in the formula for $\mathcal{G}_{B,A}^\dagger$ yields:

$$\frac{\delta E}{\delta m_A} = \langle 2 \frac{\delta \mathcal{L}_B^\dagger}{\delta m_A} \mathcal{L}_B^{-1\dagger} e_B^0, u_B^0 \rangle_B = \langle g_{B,A}, u_B^0 \rangle_B$$

$$\text{with } \lambda_B = \mathcal{L}_B^{-1\dagger} e_B^0 \text{ or } \mathcal{L}_B^\dagger \lambda_B = e_B^0 \text{ and } g_{B,A} = 2 \left[\frac{\delta \mathcal{L}^\dagger}{\delta m} \right]_{B,A} \lambda_B$$

479 (3.20)

480 The quantify $\delta \mathcal{L}_B^\dagger / \delta m_A$ has the (A, B) independent variables reversed with respect to $\delta \mathcal{L}_A / \delta m_B$.

481 However, since the Dirac function is symmetric in (A, B) , the only effect is to change the

482 independent variables in the rest of the operator from A to B .

483 In many practical cases, we will want to consider the error E_C associated with a receiver point R :

$$E_R \equiv \int [u_R^{obs} - u_R]^2 dt_R$$

484 (3.21)

485 The total error is then the superposition of the individual errors, its Fréchet derivative is the
486 superposition of individual derivatives, and λ_B is a superposition of individual $\lambda_{B,R}$'s

$$E_T = \int E_R d^3x_R \quad \text{and} \quad \frac{\delta E_T}{\delta m_A} = \int \frac{\delta E_R}{\delta m_A} d^3x_R \quad \text{and} \quad \lambda_B = \int \lambda_{B,R} d^3x_R$$

487 (3.22)

488 Inserting this definition of $\lambda_{B,R}$ into the differential equation for λ_B yields:

$$\mathcal{L}_B^\dagger \lambda_B - e^0(\mathbf{x}_R, t) = 0$$

$$\int \mathcal{L}_B^\dagger \lambda_{B,R} d^3x_R - \int e^0(\mathbf{x}_R, t) \delta(\mathbf{x}_B - \mathbf{x}_R) d^3x_R = 0$$

$$\int \{ \mathcal{L}_B^\dagger \lambda_{B,R} - e^0(\mathbf{x}_R, t) \delta(\mathbf{x}_B - \mathbf{x}_R) \} d^3x_R = 0$$

489 (3.23)

490 The presumption that this equation holds irrespective of the volume over which the error is
491 defined implied that the integrand is zero, so:

$$\mathcal{L}_B^\dagger \lambda_{B,R} = e(\mathbf{x}_R, t) \delta(\mathbf{x}_B - \mathbf{x}_R)$$

492 (3.24)

493 Thus, each $\lambda_{B,R}$ corresponds to a point source at \mathbf{x}_R with the time function of the error at that
494 point. Similarly, if we define $g_{B,A,R} \equiv 2[\delta\mathcal{L}^\dagger/\delta m]_{B,A} \lambda_{B,R}$, then a procedure analogous to the
495 one above can be used to show that:

$$\frac{\delta E_R}{\delta m_A} = \langle u_B^0, g_{B,,A,R} \rangle_B$$

496 (3.25)

497 These formula are very similar to the partial derivate case derived previously.

498 4. An Example Using the Scalar Wave Equation

499 4.1. The Partial Derivative of the Field With Respect to a Model Parameter. In the first part of
 500 this derivation, we pursue the strategy of explicitly calculating $u_R(m)$, where R is a receiver
 501 point and m is a scalar parameter, using the Born approximation. When then differentiate it to
 502 find the derivative $\partial u_R / \partial m|_{m=0}$, and use this derivative to infer $\partial E_T / \partial m|_{m=0}$. The advantage
 503 of this approach is that it allows terms in the formula for $\partial E_T / \partial m$ to be interpreted in terms of
 504 scattering interactions.

505 The scalar wave equation for an isotropic medium with constant slowness s_0 and a source that is
 506 spatially-localized at \mathbf{x}_S and has time function $f(t)$ is:

$$s_0^2 \ddot{u}_R^0 - \nabla^2 u_R^0 = \delta(\mathbf{x}_R - \mathbf{x}_S) f(t_R)$$

507 (4.1)

508 It has solution:

$$u_R^0 = \frac{f(t \pm T_{RS})}{4\pi R_{RS}} \quad \text{with } R_{RS} = |\mathbf{x}_R - \mathbf{x}_S| \quad \text{and } T_{RS} = s_0 R_{RS}$$

509 (4.2)

510 Here R_{RS} is the distance between \mathbf{x}_R and \mathbf{x}_S and T_{RS} is the corresponding travel time. The initial
 511 condition that u^0 has a quiescent past selects the forward-in-time solution ($-$ of the \pm) and the
 512 condition that it has a quiescent future selects the backwards-in-time solution ($+$ of the \pm).

513 Suppose that the slowness of the medium has the form $s_R = s_0 + \delta s_R$ where s_0 is a constant
 514 background level and δs_R is small perturbation representing spatially variable heterogeneities.

515 The quantity s_R^2 , which appears in the wave equation, is approximately:

$$s_R^2 = s_0^2 \left(1 + \frac{\delta s_R}{s_0}\right)^2 \approx s_0^2 \left(1 + 2 \frac{\delta s_R}{s_0}\right) = s_0^2 + 2s_0 \delta s_R$$

516 (4.5)

517 The corresponding scalar field is $u_R = u_R^0 + \delta u_R$, where u_R^0 solves the constant-slowness wave
 518 equation and where δu arises because the slowness field is slightly heterogeneous. Inserting this
 519 representation into the wave equation, keeping terms only to first order, and subtracting out the
 520 homogenous equation yields the Born approximation:

$$(s_0^2 + 2s_0 \delta s_R) (\dot{u}_R^0 + \delta \ddot{u}_R) - \nabla_R^2 (u_R^0 + \delta u_R) = \delta(\mathbf{x}_R - \mathbf{x}_S) f(t_R)$$

$$s_0^2 \ddot{u}_R^0 + 2s_0 \ddot{u}_R^0 \delta s_R + s_0^2 (\ddot{u}_R^0 + \delta \ddot{u}_R) - \nabla_R^2 u_R^0 - \nabla_R^2 \delta u_R = \delta(\mathbf{x}_R - \mathbf{x}_S) f(t_R)$$

$$s_0^2 \delta \ddot{u}_R - \nabla_R^2 \delta u_R = -2s_0 \ddot{u}_R^0 \delta s_R$$

521 (4.6)

522 The field perturbation δu_R solves a constant-slowness wave equation with a complicated source
 523 term. Now suppose that we consider appoint-like heterogeneity of strength m localized at
 524 position \mathbf{x}_H :

$$\delta s_R = m \delta(\mathbf{x}_R - \mathbf{x}_H)$$

525 (4.7)

526 Substituting this expression into the Born approximation yields:

$$s_0^2 \delta \ddot{u} - \nabla^2 \delta u = -2s_0 m \ddot{u}_R^0 \delta(\mathbf{x}_R - \mathbf{x}_H)$$

527 (4.8)

528 This is a constant-slowness wave equation and has solution:

$$\delta u_R = -2s_0 m \frac{\ddot{u}^0(\mathbf{x}_H, t_R - T_{RH})}{4\pi R_{RH}}$$

529 (4.9)

530 Differentiating u with respect to m yields:

$$\frac{\partial u_R}{\partial m} = \frac{\partial}{\partial m} \delta u_R = -2s_0 \frac{\ddot{u}^0(\mathbf{x}_H, t_R - T_{RH})}{4\pi R_{RH}}$$

531 (4.10)

532 4.2. The Partial Derivative of Error With Respect to a Model Parameter. Now suppose we have

533 an observation u_R^{obs} for some fixed observer location R . The error E is defined as:

$$E_R = \int (e_R^0)^2 dt_R \quad \text{with} \quad e_R^0 = u_R^{obs} - u_R^0$$

534 (4.11)

535 The derivative is:

$$\frac{\partial E_R}{\partial m} = -2 \int e_R^0 \frac{\partial u_R}{\partial m} dt$$

536 (4.12)

537 Inserting Equation (4.10) yields:

$$\begin{aligned} \frac{\partial E_R}{\partial m} &= 4s_0 \frac{1}{4\pi R_{RH}} \int e_R^0 \ddot{u}^0(\mathbf{x}_H, t_R - T_{RH}) dt_R \\ &= 4s_0 \frac{1}{4\pi R_{RH}} \frac{1}{4\pi R_{HS}} \int e_R^0 \ddot{f}(t_R - T_{RH} - T_{HS}) dt_R \\ &= 4s_0 \frac{1}{4\pi R_{RH}} \frac{1}{4\pi R_{HS}} \int \ddot{e}_R^0 f(t_R - T_{RH} - T_{HS}) dt_R \end{aligned}$$

538 (4.13)

539 The last form is derived by noting that the integral is an inner product and that the time
 540 derivative, which is self-adjoint, can be moved from f to $(u^{obs} - u)$. The source time function f
 541 is propagated outward from the source, scattered off the heterogeneity, and then propagated to
 542 the observer (Figure 1A) , where it is “correlated” (time-integrated) with the second derivative \ddot{e}
 543 of the error.

544 We now apply the transformation of variables $t_A = t_R - T_{RH}$ to the integral in Equation (4.13).

545 Then:

$$\frac{\partial E_R}{\partial m} = 4s_0 \frac{1}{4\pi R_{RH}} \frac{1}{4\pi R_{HS}} \int \ddot{e}(\mathbf{x}_R, t_A + T_{RH}) f(t_A - T_{HS}) dt_A$$

546 (4.14)

547 In this version, the source time function is propagated forward in time from the source to the
 548 heterogeneity and the error is propagated backward in time from the observation point to the
 549 heterogeneity (Figure 1B), and the two are then correlated. We have achieved a form that is very
 550 reminiscent of formula derived using the Adjoint Method, without explicitly applying adjoint
 551 methodology. Or rather, we *have* applied adjoint methodology without recognizing that we have
 552 done so; compare with the derivation of the Green function adjoint in Equation (A.5).

553 4.3. Computation of $\partial E/\partial m|_{m=0}$ Using the Adjoint Method. The wave equation operator is
 554 self-adjoint, so the Adjoint field equation (see Equation 2.6) and its solution are:

$$\mathcal{L}_A^\dagger \lambda_{A,R} = \left(s_0^2 \frac{\partial^2}{\partial t_A^2} - \nabla_A^2 \right) \lambda_{A,R} = e^0(\mathbf{x}_R, t_A) \delta(\mathbf{x}_A - \mathbf{x}_R)$$

$$\lambda_{A,R} = \frac{e^0(t_A + T_{AR})}{4\pi R_{AR}}$$

555 (4.15)

556 Here we have selected the quiescent future form of solution (+ of the \pm in Equation 4.2). The
 557 derivative of the wave equation operator is also self-adjoint and is:

$$\frac{\partial \mathcal{L}_A}{\partial m} = \frac{\partial \mathcal{L}_A^\dagger}{\partial m} = 2s_0 \delta(\mathbf{x}_A - \mathbf{x}_H) \frac{\partial^2}{\partial t_A^2}$$

558 (4.16)

559 so

$$h_{A,R} = 2 \frac{\partial \mathcal{L}_A^\dagger}{\partial m} \lambda_{A,R} = 2s_0 \delta(\mathbf{x}_A - \mathbf{x}_H) \frac{\ddot{e}^0(t_A + T_{AR})}{4\pi R_{AR}}$$

560 (4.17)

561 The unperturbed field satisfies:

$$\mathcal{L}_A u_A^0 = \left(s_0^2 \frac{\partial^2}{\partial t_A^2} - \nabla_A^2 \right) = \delta(\mathbf{x}_A - \mathbf{x}_S) f(t_S) \quad \text{so} \quad u_A^0 = \frac{f(t_A - T_{AS})}{4\pi R_{AS}}$$

562 (4.18)

563 Here we have selected the quiescent past form of solution (– of the \pm in Equation 4.2).

564 Inserting this expression into Equation (2.7) yields an expression for the derivative:

$$\begin{aligned} \frac{\partial E_R}{\partial m} &= \langle h_{A,R}, u_A^0 \rangle_A = \langle 2s_0 \delta(\mathbf{x}_A - \mathbf{x}_H) \frac{\ddot{e}^0(t_A + T_{AR})}{4\pi R_{AR}}, \frac{f(t_A - T_{AS})}{4\pi R_{AS}} \rangle_A \\ &= 4s_0 \frac{1}{4\pi R_{RH}} \frac{1}{4\pi R_{HS}} \int \ddot{e}^0(t_A + T_{RH}) f(t_A - T_{HS}) dt_A \end{aligned}$$

565 (4.19)

566 This is the same formula that was derived in Equation (4.14) using the Born approximation. The
 567 spatial pattern of the derivative is axially-symmetric about a line drawn through source and
 568 receiver and has the form of a series of concentric ellipses of alternating sign, with foci at the
 569 source and receiver (Figure 2). The ellipses represent surfaces of equal travel time from source
 570 to heterogeneity to receiver. The amplitude of the derivative varies across the surface of an
 571 ellipse, because it depends upon the product of the source-to-heterogeneity and heterogeneity-to-
 572 receiver distances, rather than their sum.

573 Zhu et al. [2009] point out an interesting link between the Adjoint Method and seismic migration
 574 [Claerbout and Doherty 1972], an imaging method commonly applied in reflection seismology.

575 In this setting, the unperturbed field, due to a source on the Earth’s surface, is down-going and
576 the perturbed field, due to heterogeneities within the Earth that scatter waves back up to the
577 Earth’s surface, is up-going. The imaging principle of seismic migration is based on the idea
578 that, when the perturbed field δu is back-propagated into the earth, and the unperturbed field u^0
579 is forward propagated into the earth, the two will arrive at a scatterer at the same time (since the
580 unperturbed field is the source of the perturbed field). A scatterer at a point \mathbf{x}_H can be detected
581 (“imaged”) by correlating δu with the \ddot{u}^0 (the source associated with u^0). This is precisely what
582 the adjoint formulation is doing: the unperturbed field is forward-propagated in Equation
583 (4.15b); the perturbed field is back-propagated in Equation (4.15c) (if we assume $e \approx \delta u^{obs}$);
584 and the two fields are time-correlated at the position of the heterogeneity in Equation 4.16.
585 Hence, migration is just using $\partial E / \partial m$ as a proxy for m^{est} (see Equation 8.4). This
586 correspondence provides a mechanism for generalizing seismic migration to more complicated
587 settings [Luo et al., 2013].

588 5. Finite Frequency Travel Time Tomography

589

590 5.1. Rationale for Finite-Frequency Measurements. Traditionally, seismic tomography has used
591 travel times based on “picks” of the onset of motion of a seismic phase on a seismogram, either
592 determined “by eye” by a human analyst or automatically with, say, a short term average - long
593 term average (STA/LTA) algorithm [Coppens, 1985]. Such travel times are easy to measure on
594 short-period seismograms but problematical at longer periods, owing to the emergent onset of the
595 waveforms. A more suitable measurement technique for these data involves cross-correlating
596 the observed seismic phase with a synthetic reference seismogram, because cross-correlation can
597 accurately determine the small time difference, say τ , between two smooth pulses. However, the

598 results of cross-correlation are dependent upon the frequency band of measurement; a phase that
599 is observed to arrive earlier than the reference phase at one frequency may well arrive later than
600 it at another. Consequently, finite-frequency travel times must be interpreted in the context of
601 the frequency band at which they are measured. Finite-frequency travel time tomography is
602 based upon a derivative $\partial\tau/\partial m$ (where m is a model parameter) than incorporates the
603 frequency-dependent behavior of cross-correlations.

604

605 5.2. Definition of Differential Travel Time. The differential travel time τ^0 between an observed
606 field $u^{obs}(t) \equiv u^{obs}(\mathbf{x}, t)$ and a predicted field $u^0(t) \equiv u^0(\mathbf{x}, t)$ is defined as the one that
607 maximizes the cross-correlation:

608

$$C(\mathbf{x}, \tau; u^0) = \int u^{obs}(t - \tau) u^0(t) dt$$

609 (5.1)

610 Since the cross-correlation is maximum at τ^0 , its first derivative is zero there:

611

$$\left. \frac{dC(\mathbf{x}, \tau; u^0)}{d\tau} \right|_{\tau^0} = 0$$

612 (5.2)

613

614 5.3. Perturbation in Travel Time due to a Perturbation in the Predicted Wave Field. Suppose that
615 the predicted field is perturbed from u^0 to $u = u^0 + \delta u$. The cross-correlation is perturbed to
616 Marquering et al. 1999]:

617

$$C(\mathbf{x}, \tau; u) = C(\mathbf{x}, \tau; u^0) + \delta C(\mathbf{x}, \tau) \quad \text{with} \quad \delta C(\mathbf{x}, \tau) = \int u^{obs}(t - \tau) \delta u(t) dt$$

618 (5.3)

619

620 This function has a maximum at, say, $\tau = \tau^0 + \delta\tau$. Expanding $C(\mathbf{x}, \tau; u)$ in a Taylor series up to

621 second order in small quantities yields:

622

$$C(\mathbf{x}, \tau; u) = C(\mathbf{x}, \tau; u^0)|_{\tau^0} + 0 + \frac{1}{2} \frac{d^2 C(\mathbf{x}, \tau; u^0)}{d\tau^2} \Big|_{\tau^0} (\delta\tau)^2 + \delta C(\mathbf{x}, \tau)|_{\tau^0} + \frac{d\delta C(\mathbf{x}, \tau)}{d\tau} \Big|_{\tau^0} \delta\tau$$

623

624 (5.4)

625 As is shown in Equation (5.2), the second term on the r.h.s. is zero. The maximum occurs where

626 the derivative is zero:

$$\frac{dC(\mathbf{x}, \tau)}{d\tau} = 0 \approx \frac{d^2 C(\mathbf{x}, \tau)}{d\tau^2} \Big|_{\tau^0} \delta\tau + \frac{d\delta C(\mathbf{x}, \tau)}{d\tau} \Big|_{\tau^0}$$

627 (5.5)

628 Solving for $\delta\tau$ yields:

$$\delta\tau \approx - \frac{d\delta C(\mathbf{x}, \tau)}{d\tau} \Big|_{\tau^0} / \frac{d^2 C(\mathbf{x}, \tau)}{d\tau^2} \Big|_{\tau^0}$$

629 (5.6)

630 The numerator is:

631

$$\frac{d\delta C}{d\tau} \Big|_{\mathbf{x}, \tau^0} = \frac{d}{d\tau} \int u^{obs}(\mathbf{x}, t - \tau) \delta u(\mathbf{x}, t) dt \Big|_{\tau^0} = - \int \dot{u}_B^{obs}(\mathbf{x}, t_B - \tau^0) \delta u(\mathbf{x}, t) dt$$

632 (5.7)

633 and the denominator is:

$$\begin{aligned} \frac{dC(\mathbf{x}, \tau)}{d\tau} &= \frac{d}{d\tau} \int u^{obs}(\mathbf{x}, t - \tau) u^0(\mathbf{x}, t) dt = - \int \dot{u}^{obs}(\mathbf{x}, t - \tau) u^0(\mathbf{x}, t) dt \\ D(\mathbf{x}, \tau^0) &\equiv \left. \frac{d^2 C(\tau^0; u_B^0)}{d\tau^2} \right|_{\tau^0} = - \left. \frac{d}{d\tau} \int \dot{u}^{obs}(\mathbf{x}, t - \tau) u^0(\mathbf{x}, t) dt \right|_{\tau^0} \\ &= \int \dot{u}^{obs}(\mathbf{x}, t + \tau^0) u^0(\mathbf{x}, t) dt \end{aligned}$$

634 (5.8)

635 Consequently, the perturbation in differential arrival time of an observer at \mathbf{x}_A satisfies:

$$\delta\tau_A = \int \left(\frac{\dot{u}^{obs}(\mathbf{x}_A, t_B + \tau^0)}{D(\mathbf{x}_A)} \right) \delta u(\mathbf{x}_A, t_B) dt_B = \langle h_{A,B}, \delta u_B \rangle_B$$

636 (5.9)

637 with

$$h_{A,B} = \frac{\dot{u}^{obs}(\mathbf{x}_A, t_B + \tau^0)}{D(\mathbf{x}_A)} \delta(\mathbf{x}_B - \mathbf{x}_A)$$

638 (5.10)

639

640 5.4. Derivative of Travel Time with Respect to a Model Parameter. According to (A.3), a

641 perturbation Δm to a structural parameter m causes a corresponding perturbation in the field:

642

$$\delta u_B = -\mathcal{L}_B^{-1} \frac{\partial \mathcal{L}_B}{\partial m} u_B^0 \Delta m$$

643 (5.11)

644 Inserting this expression into the formula for $\delta\tau$ yields:

$$\delta\tau_A = \langle h_{A,B}, \delta u_B \rangle_B = - \langle h_{A,B}, \mathcal{L}_B^{-1} \frac{\partial \mathcal{L}_B}{\partial m} u_B^0 \rangle_B \Delta m = - \langle \mathcal{L}_B^{-1\dagger} h_{A,B}, \frac{\partial \mathcal{L}_B}{\partial m} u_B^0 \rangle_B \Delta m$$

$$\frac{\partial \tau_A}{\partial m} = - \langle H_{A,B}, \frac{\partial \mathcal{L}_B}{\partial m} u_B^0 \rangle_A \quad \text{with} \quad \mathcal{L}_B^\dagger H_{A,B} = h_{A,B}$$

645 (5.12)

646

647 Note that the adjoint differential equation has a source term that is localized at the receiver point

648 A and has a source time function proportional to $\dot{u}^{obs}(\mathbf{x}_A)$.

649

650 5.6. Fréchet Derivative. The corresponding Fréchet derivative combines $\delta\tau(\mathbf{x}_A) = \langle h_{A,B}, \delta u_B \rangle_B$

651 with

652

$$\delta u_B = \left\langle \left[\frac{\delta u}{\delta m} \right]_{B,C}, \delta m_C \right\rangle \quad \text{with} \quad G_{B,C} \equiv \left[\frac{\delta u}{\delta m} \right]_{B,C} = -\mathcal{L}_B^{-1} \left[\frac{\delta \mathcal{L}}{\delta m} \right]_{B,C} u_B^0$$

653 (5.13)

654 to yield:

$$\delta\tau(\mathbf{x}_A) = \langle h_{A,B}, \langle G_{B,C}, \delta m_C \rangle_C \rangle_B = \langle \langle h_{A,B}, G_{B,C} \rangle_B, \delta m_C \rangle_C$$

655 (5.14)

656 from whence we conclude:

$$\left[\frac{\delta \tau}{\delta m} \right]_{A,C} = \langle h_{A,B}, G_{B,C} \rangle_B = - \langle H_{A,B}, \left[\frac{\delta \mathcal{L}}{\delta m} \right]_{B,C} u_B^0 \rangle_B$$

657 (5.16)

658

659 with, as before,

$$\mathcal{L}_B^\dagger H_{A,B} = h_{A,B}$$

660 (5.17)

661

662 6. An Example Using the Scalar Wave Equation

663 6.1. Choice of the Observed Field. As in Section 4, we consider an isotropic medium with a

664 homogeneous background slowness s_0 containing a *test* point heterogeneity of strength m

665 located at position \mathbf{x}_H . This scenario allows us to address how the alignment changes as the test

666 heterogeneity is moved to different positions relative to the source and observer The observed

667 field is taken to be identical to the direct wave in the absence of the heterogeneity; that is, when

668 $m = 0$. Since the $u^{obs}(\mathbf{x}_R, t)$ and $u^0(\mathbf{x}_R, t)$ already align, we can set $\tau^0 = 0$. The differential

669 equation is $\mathcal{L}(m) u = \delta(\mathbf{x} - \mathbf{x}_S) f(t)$, where:

$$\mathcal{L} = \mathcal{L}^\dagger = s_0^2 \frac{\partial^2}{\partial t^2} + 2s_0 m \delta(\mathbf{x} - \mathbf{x}_H) \frac{\partial^2}{\partial t^2} - \nabla^2$$

670 (6.1)

671

672 The source time function $f(t)$ is assumed to be band-limited between angular frequencies ω_1

673 and ω_2 , e.g.:

$$f(t) = \text{sinc}(\omega_1 t) - \text{sinc}(\omega_2 t)$$

674 (6.2)

675 The observed field at the receiver is the direct field u^0 ; that is:

$$u_R^{obs} = \frac{f(t_R - T_{SR})}{4\pi R_{SR}}$$

676 (6.3)

677

678 6.2. The Partial Derivative of Travel Time With Respect to the Model. Our goal is to construct

679 $\partial\tau/\partial m$ associated with a point heterogeneity at \mathbf{x}_H . First, we construct the function H_A , which

680 involves back-propagating, via the adjoint equation, the observed field at the receiver point \mathbf{x}_R to

681 an arbitrary point \mathbf{x}_A :

$$\mathcal{L}^\dagger H = \frac{\dot{u}_R^{obs}}{D(\mathbf{x}_R)} \delta(\mathbf{x} - \mathbf{x}_R) \quad \text{or} \quad H_A = -\frac{1}{D(\mathbf{x}_R)} \frac{\dot{f}(t_A - T_{SR} + T_{RA})}{4\pi R_{SR} 4\pi R_{RA}}$$

682 (6.4)

683

684 Second, we construct the function $G_{A,H}$, also for an arbitrary point \mathbf{x}_A :

$$G_{A,H} = -\frac{\partial\mathcal{L}}{\partial m} u^0 = -2s_0 \delta(\mathbf{x}_A - \mathbf{x}_H) \frac{\partial^2}{\partial t^2} \frac{f(t - T_{SA})}{4\pi R_{SA}} = -2s_0 \delta(\mathbf{x}_A - \mathbf{x}_H) \frac{\ddot{f}(t - T_{SA})}{4\pi R_{SA}}$$

685 (6.5)

686 Finally, we combine H_A and $G_{A,H}$ via an inner product to construct the partial derivative:

$$\left. \frac{\partial\tau}{\partial m} \right|_{\mathbf{x}_H} = \langle H_A, G_{A,H} \rangle_A = \left\langle -\frac{1}{D(\mathbf{x}_R)} \frac{\dot{f}(t_A - T_{SR} + T_{RA})}{4\pi R_{SR} 4\pi R_{RA}}, -2s_0 \delta(\mathbf{x}_A - \mathbf{x}_T) \frac{\ddot{f}(t_A - T_{SA})}{4\pi R_{SA}} \right\rangle_A$$

$$\begin{aligned}
&= \frac{2s_0}{D(\mathbf{x}_R)} \frac{1}{4\pi R_{SR} 4\pi R_{RH} 4\pi R_{SH}} \int \dot{f}(t_A - T_{SR} + T_{RH}) \ddot{f}(t_A - T_{SH}) dt_A \\
&= \frac{2s_0}{D(\mathbf{x}_R)} \frac{1}{4\pi R_{SR} 4\pi R_{RH} 4\pi R_{SH}} \int \dot{f}(t - \Delta T) \ddot{f}(t) dt
\end{aligned}$$

687 (6.6)

688 The last form uses the transformation of variables $t = t_A - T_{SH}$ where:

$$\Delta T = T_{SR} - T_{RH} - T_{SH} = T_{SR} - (T_{SH} + T_{RH})$$

689 (6.7)

690 The quantity ΔT represents the difference in travel times between the direct (S - R) and scattered

691 (S - H - R) paths. The quantity $D(\mathbf{x}_R)$ is given by:

$$\begin{aligned}
D(\mathbf{x}_R) &= \int \ddot{u}^{obs}(\mathbf{x}_R, t) u^0(\mathbf{x}_R, t) dt = \frac{1}{4\pi R_{SR} 4\pi R_{SR}} \int \ddot{f}(t) f(t) dt \\
&= -\frac{1}{(4\pi R_{SR})^2} \int [\dot{f}(t)]^2 dt
\end{aligned}$$

692 (6.8)

693 We have used the anti-self-adjoint property of the d/dt operator to simplify the last integral.

694 6.3. Analysis. The derivative $\partial\tau/\partial m$ is axially symmetric about the (S - R) line, since R_{SR} and

695 R_{RH} depend only on the perpendicular distance r of \mathbf{x}_H from the line. Sliced perpendicular to the

696 line, $\partial\tau/\partial m$ is “doughnut-shaped”.

697 The derivative $\partial\tau_A/\partial m = 0$ whenever $\Delta T = 0$. This behavior follows from d/dt being an anti-

698 self-adjoint operator, since any quantity equal to its negative is zero:

$$\int \dot{f}(t) \ddot{f}(t) dt = - \int \ddot{f}(t) \dot{f}(t) dt = - \int \dot{f}(t) \ddot{f}(t) dt = 0$$

699 (6.9)

700

701 The time difference ΔT is zero when the test heterogeneity is between S and R and on the $(S-R)$
 702 line, so $\partial\tau/\partial m = 0$ in this case. This zero makes the ‘hole’ in the center of the doughnut’.

703 Now consider an oscillatory, band-limited source time function with a characteristic period P .

704 Suppose we construct the elliptical volume surrounding the points \mathbf{x}_S and \mathbf{x}_R for which $\Delta T <$

705 $P/2$. The time integral in (F.2) will have the same sign everywhere in this volume, as will

706 $\partial\tau/\partial m$. This region defines the “banana.” The banana is thinner for short periods than for long

707 periods (Figure 4).

708 Moving away from the $(S-R)$ line along its perpendicular, the time integral, and hence the

709 derivative, oscillates in sign, as the $\dot{f}(t - \Delta T)$ and $\ddot{f}(t)$ factors beat against one another. The

710 derivative also decreases in amplitude (since the factors R_{RH} and R_{SH} grow with distance).

711 Consequently, the central banana is surrounded by a series of larger, but less intense, bananas of

712 alternating sign.

713 7. Adjoint Method Applied to the Cross-Convolution Method

714 7.1. Definition. The cross-convolution method [Menke and Levin, 2003] is used to invert shear

715 wave splitting and receiver function data for Earth structure [e.g. Bodin et al. 2014]. It is

716 especially useful for extracting structural information from differences between the several

717 components of a P or S wave because, unlike other waveform modeling approaches, it does not

718 require knowledge of the source time function. It compares two different components u_i^{obs} and
 719 u_j^{obs} observed at the same position with their predictions u_i and u_j , using the measure:

$$\Psi(m) = \langle w_A(m), w_A(m) \rangle_A \text{ with } w_A(m) = (\Omega u_j^{obs}) * (\Omega u_i(m)) - (\Omega u_i^{obs}) * (\Omega u_j(m))$$

720 (7.1)

721

722 Here $\Omega(t)$ is a window function that selects a particular seismic phase, such as the P wave, from
 723 the time series. The cross-convolution measure $\Psi(m)$ is a function of Earth structure, as
 724 quantified by a parameter m . Because $\Psi(m)$ scales with the amplitude of the predicted
 725 waveform, determining the model parameters by minimizing $\Phi(m) \equiv \Psi/P$, where $P(m)$ is total
 726 power, is preferable to determining them by minimizing $\Psi(m)$. The total power is given by:

$$P(m) = \langle \Omega \mathbf{u}(m), \Omega \mathbf{u}(m) \rangle_A$$

727 (7.2)

728

729 The partial derivative of $\Phi = \Psi/P$ with respect to a model parameter is calculated using the
 730 chain rule:

$$\left. \frac{\partial \Phi}{\partial m} \right|_{m_0} = \left. \frac{\partial \Psi P^{-1}}{\partial m} \right|_{m_0} = \left. \frac{\partial \Psi}{\partial m} \right|_{m_0} P_0^{-1} - \Psi_0 \left. \frac{\partial P}{\partial m} \right|_{m_0} P_0^{-2}$$

731 (7.3)

732 As we show below, the derivatives $\partial \Psi / \partial m$ and $\partial P / \partial m$ can be derived using Adjoint Methods.

733 G.2. The Partial Derivative of Power With Respect to Model Parameter. The $\partial P/\partial m$ derivative
 734 is:

$$\begin{aligned} \frac{\partial P}{\partial m}\Big|_{m_0} &= 2 \langle \Omega_A \mathbf{u}_A(m), \Omega \frac{\partial \mathbf{u}_A}{\partial m} \rangle_A = 2 \langle \Omega_A^2 \mathbf{u}_A(m), \frac{\partial \mathbf{u}_A}{\partial m} \rangle_A \\ &= -2 \langle \Omega^2 \mathbf{u}_A^0(m), \mathcal{L}_A^{-1} \frac{\partial \mathcal{L}_A}{\partial m} \mathbf{u}_A^0 \rangle_A = -2 \langle \frac{\partial \mathcal{L}_A^\dagger}{\partial m} \mathcal{L}_A^{\dagger-1} \Omega_A^2 \mathbf{u}_A^0, \mathbf{u}_A^0 \rangle_A \\ \text{or } \frac{\partial P}{\partial m}\Big|_{m_0} &= -2 \langle \frac{\partial \mathcal{L}_A^\dagger}{\partial m} \boldsymbol{\xi}_A, \mathbf{u}_A^0 \rangle_A \quad \text{with} \quad \mathcal{L}_A^\dagger \boldsymbol{\xi}_A = \Omega_A^2 \mathbf{u}_A^0 \end{aligned}$$

735 Here, $\boldsymbol{\xi}_A$ is the adjoint field associated with the power derivative. We consider the total power P
 736 to be the sum of the power P^R associated with individual observation points \mathbf{x}_R . The
 737 corresponding adjoint field $\boldsymbol{\xi}_A^R$ satisfies:

$$\mathcal{L}_A^\dagger \boldsymbol{\xi}_A^R = \Omega_R^2 \mathbf{u}^0(\mathbf{x}_R, t) \delta(\mathbf{x}_A - \mathbf{x}_R)$$

738 We now consider a point density perturbation $\rho = m\delta(\mathbf{x} - \mathbf{x}_H)$ located at \mathbf{x}_H . The derivative of
 739 the adjoint operator is:

$$\frac{\partial \mathcal{L}_A^\dagger}{\partial m} = \delta(\mathbf{x}_A - \mathbf{x}_H) \begin{bmatrix} 1 & 0 & 0 \\ 0 & 1 & 0 \\ 0 & 0 & 1 \end{bmatrix} \frac{\partial^2}{\partial t^2}$$

740 The power derivative is:

$$\frac{\partial P}{\partial m}\Big|_{m_0} = -2 \int \boldsymbol{\xi}^R(\mathbf{x}_H, t_H) \cdot \dot{\mathbf{u}}^0(\mathbf{x}_H, t_H) dt_H$$

741 G.3. The derivative $\partial \Psi/\partial m$. The cross-convolution function w is constructed from the predicted
 742 wave field \mathbf{u} through a linear operator \mathcal{W} that is independent of the model parameter:

$w(m) = \mathcal{W} \Omega \mathbf{u}(m)$ with $\mathbf{u} = [\dots \mathbf{u}_i, \dots, \mathbf{u}_j, \dots]$ and

and $\mathcal{W} = (\mathbf{U} \star)$ with $\mathbf{U} = [\dots \Omega u_j^{obs}, 0, -\Omega u_i^{obs}, \dots]$

743 The adjoint of \mathcal{W} is the cross-correlation operator $\mathcal{W}^\dagger = (\mathbf{U}^T \star)$. The partial derivative of Ψ

744 with respect to a model parameter m is:

$$\left. \frac{\partial \Psi}{\partial m} \right|_{m_0} = \frac{\partial}{\partial m} \langle w_A, w_A \rangle_A = \langle 2w_A^0, \left. \frac{\partial w_A}{\partial m} \right|_{m_0} \rangle_A$$

745

$$= \langle 2\mathcal{W}_A \Omega_A \mathbf{u}_A^0, \mathcal{W}_A \Omega_A \left. \frac{\partial \mathbf{u}_A}{\partial m} \right|_{m_0} \rangle_A = \langle -2\mathcal{W}_A \Omega_A \mathbf{u}_A^0, \mathcal{W}_A \Omega_A \mathcal{L}_A^{-1} \left. \frac{\partial \mathcal{L}_A}{\partial m} \mathbf{u}_A^0 \right|_A \rangle_A$$

$$= \langle -2 \left. \frac{\partial \mathcal{L}_A^\dagger}{\partial m} \mathcal{L}_A^{\dagger-1} \Omega_A \mathcal{W}_A^\dagger \mathcal{W}_A \Omega_A \mathbf{u}_A^0 \right|_A \rangle_A = \langle -2 \left. \frac{\partial \mathcal{L}_A^\dagger}{\partial m} \boldsymbol{\lambda}_A, \mathbf{u}_A^0 \right|_A \rangle_A$$

746 (7.4)

747 Here $\boldsymbol{\lambda}_A$ is an adjoint field that satisfies:

$$\mathcal{L}_A^\dagger \boldsymbol{\lambda}_A = \boldsymbol{\varphi}_A \quad \text{with} \quad \boldsymbol{\varphi}_A \equiv \Omega_A \mathcal{W}_A^\dagger \mathcal{W}_A \Omega_A \mathbf{u}_A^0 = \Omega_A (\mathbf{U}_A^T \star \mathbf{U}_A) \star (\Omega_A \mathbf{u}_A^0) = \Omega_A \mathbf{X}_A \star (\Omega_A \mathbf{u}_A^0)$$

748

$$\text{with } \mathbf{X}_A \equiv \begin{bmatrix} \ddots & \vdots & & & \vdots & & \vdots & \ddots \\ \dots & 0 & & 0 & & 0 & & \dots \\ \dots & 0 & \{\Omega_A \mathbf{u}_{A,j}^{obs} \star \Omega_A \mathbf{u}_{A,j}^{obs}\} & & -\{(\Omega_A \mathbf{u}_{A,j}^{obs}) \star (\Omega_A \mathbf{u}_{A,i}^{obs})\} & & 0 & \dots \\ \dots & 0 & 0 & & 0 & & 0 & \dots \\ \dots & 0 & -(\Omega_A \mathbf{u}_{A,i}^{obs}) \star (\Omega_A \mathbf{u}_{A,j}^{obs}) & & (\Omega_A \mathbf{u}_{A,i}^{obs}) \star (\Omega_A \mathbf{u}_{A,i}^{obs}) & & 0 & \dots \\ \dots & 0 & 0 & & 0 & & 0 & \dots \\ \ddots & \vdots & & & \vdots & & \vdots & \ddots \end{bmatrix}$$

749 (7.5)

750

751 Here $w_A^0 \equiv w_A(m_0)$. The source term of the adjoint equation involves cross-correlations of
 752 windowed components of the observed field. As with previous cases, we can view the λ_A as the
 753 superposition of contributions λ_A^R of many observation points \mathbf{x}_R . The adjoint equation
 754 corresponding to a single observation point is:

$$\mathcal{L}_A^\dagger \lambda_A^R = \boldsymbol{\varphi}^R(\mathbf{x}_R, t_A) \delta(\mathbf{x}_A - \mathbf{x}_R)$$

755 (7.6)

756 We again consider the special case of a point density heterogeneity, so that $\partial \mathcal{L}_A^\dagger / \partial m =$
 757 $\delta(\mathbf{x}_A - \mathbf{x}_H) (\partial^2 / \partial t^2) \mathbf{I}$ (where \mathbf{I} is the identity matrix). The partial derivative is then:

$$\left. \frac{\partial \Psi^R}{\partial m} \right|_{m_0} = \langle -2 \frac{\partial \mathcal{L}_A^\dagger}{\partial m} \lambda_A^R, \mathbf{u}_A^0 \rangle_A = \langle -2 \delta(\mathbf{x}_A - \mathbf{x}_H) \lambda_A^R, \dot{\mathbf{u}}_A^0 \rangle_A = -2 \int \lambda^R(\mathbf{x}_H, t_H) \cdot \dot{\mathbf{u}}(\mathbf{x}_H, t_H) dt_H$$

758 (7.7)

759

760 7.4. Derivatives With Respect to Lamé Parameters. Assuming a perturbation of the form

761 $\lambda = m \delta(\mathbf{x}_A - \mathbf{x}_H)$ the λ derivative of the adjoint wave operator is:

762

$$\frac{\partial \mathcal{L}^\dagger}{\partial m} = -\delta \begin{bmatrix} \frac{\partial^2}{\partial x^2} & \frac{\partial^2}{\partial x \partial y} & \frac{\partial^2}{\partial x \partial z} \\ \frac{\partial^2}{\partial x \partial y} & \frac{\partial^2}{\partial y^2} & \frac{\partial^2}{\partial y \partial z} \\ \frac{\partial^2}{\partial x \partial z} & \frac{\partial^2}{\partial y \partial z} & \frac{\partial^2}{\partial z^2} \end{bmatrix} - \begin{bmatrix} \frac{\partial \delta}{\partial x} \frac{\partial}{\partial x} & \frac{\partial \delta}{\partial x} \frac{\partial}{\partial y} & \frac{\partial \delta}{\partial x} \frac{\partial}{\partial z} \\ \frac{\partial \delta}{\partial y} \frac{\partial}{\partial x} & \frac{\partial \delta}{\partial y} \frac{\partial}{\partial y} & \frac{\partial \delta}{\partial y} \frac{\partial}{\partial z} \\ \frac{\partial \delta}{\partial z} \frac{\partial}{\partial x} & \frac{\partial \delta}{\partial z} \frac{\partial}{\partial y} & \frac{\partial \delta}{\partial z} \frac{\partial}{\partial z} \end{bmatrix}$$

763 (7.8)

764

765

766 Here the δ 's are abbreviations for the Dirac function $\delta(\mathbf{x}_A - \mathbf{x}_H)$. Assuming a perturbation of the

767 form $\mu = m \delta(\mathbf{x}_A - \mathbf{x}_H)$ the μ derivative of the adjoint wave operator is:

768

$$\frac{\partial \mathcal{L}^\dagger}{\partial m} = -\delta \begin{bmatrix} 2 \frac{\partial^2}{\partial x^2} + \frac{\partial^2}{\partial y^2} + \frac{\partial^2}{\partial z^2} & \frac{\partial^2}{\partial x \partial y} & \frac{\partial^2}{\partial x \partial z} \\ \frac{\partial^2}{\partial x \partial y} & \mu \frac{\partial^2}{\partial x^2} + 2 \frac{\partial^2}{\partial y^2} + \frac{\partial^2}{\partial z^2} & \frac{\partial^2}{\partial y \partial z} \\ \frac{\partial^2}{\partial x \partial z} & \frac{\partial^2}{\partial y \partial z} & \frac{\partial^2}{\partial x^2} + \mu \frac{\partial^2}{\partial y^2} + 2 \frac{\partial^2}{\partial z^2} \end{bmatrix}$$

769

$$- \begin{bmatrix} 2 \frac{\partial \delta}{\partial x} \frac{\partial}{\partial x} + \frac{\partial \delta}{\partial y} \frac{\partial}{\partial y} + \frac{\partial \delta}{\partial z} \frac{\partial}{\partial z} & \frac{\partial \delta}{\partial y} \frac{\partial}{\partial x} & \frac{\partial \delta}{\partial z} \frac{\partial}{\partial x} \\ \frac{\partial \delta}{\partial x} \frac{\partial}{\partial y} & \frac{\partial \delta}{\partial x} \frac{\partial}{\partial x} + 2 \frac{\partial \delta}{\partial y} \frac{\partial}{\partial y} + \frac{\partial \delta}{\partial z} \frac{\partial}{\partial z} & \frac{\partial \delta}{\partial z} \frac{\partial}{\partial y} \\ \frac{\partial \delta}{\partial x} \frac{\partial}{\partial z} & \frac{\partial \delta}{\partial y} \frac{\partial}{\partial z} & \frac{\partial \delta}{\partial x} \frac{\partial}{\partial x} + \frac{\partial \delta}{\partial y} \frac{\partial}{\partial y} + 2 \frac{\partial \delta}{\partial z} \frac{\partial}{\partial z} \end{bmatrix}$$

770 (7.9)

771

772

773 The inner products for $\partial\Psi/\partial m$ and $\partial\Psi/\partial m$ include both Dirac delta functions and their spatial

774 derivatives. For instance, in the λ case:

$$\left. \frac{\partial \Psi}{\partial m} \right|_{m_0=0} = \langle -2 \frac{\partial \mathcal{L}_A^\dagger}{\partial m} \lambda_A, \mathbf{u}_A^0 \rangle_A$$

775

$$\begin{aligned}
&= 2 \langle \delta(\mathbf{x}_A - \mathbf{x}_H) \frac{\partial^2 \lambda_{A,x}}{\partial x^2}, u_{A,x}^0 \rangle_A + 2 \left\langle \frac{\partial}{\partial x} \delta(\mathbf{x}_A - \mathbf{x}_H) \right\rangle \frac{\partial \lambda_{A,x}}{\partial x}, u_{A,x}^0 \rangle_A + \dots \\
&= 2 \int \frac{\partial^2 \lambda_{H,x}}{\partial x^2} u_{H,x}^0 dt_H - 2 \int \frac{\partial}{\partial x} \left\{ \frac{\partial \lambda_{A,x}}{\partial x} u_{H,x}^0 \right\} dt_H \dots \\
&= 2 \int \frac{\partial^2 \lambda_{H,x}}{\partial x^2} u_{H,x}^0 dt_H - 2 \int \frac{\partial^2 \lambda_{H,x}}{\partial x^2} u_{H,x}^0 dt_H - 2 \int \frac{\partial \lambda_{A,x}}{\partial x} \frac{\partial u_{H,x}^0}{\partial x} dt_H \dots
\end{aligned}$$

776 (7.10)

777

778 Here we have used the rule $\int f(x_A) \{d\delta(x_A - x_H)/dx_A\} dx_A = -df(x_H)/dx_H$. Thus, $\partial\Psi/\partial m$
779 and $\partial\Psi/\partial m$ involve temporal correlations between spatial gradients of both adjoint and
780 unperturbed fields. The inner product can be succinctly written:

$$\langle -2 \frac{\partial \mathcal{L}_A^\dagger}{\partial m} \boldsymbol{\lambda}_A, \mathbf{u}_A^0 \rangle = -2 \sum_i \sum_j \int [\mathcal{D}]_{ij} \{[\boldsymbol{\lambda}_H]_j [\mathbf{u}_H^0]_i\} dt_H$$

781 (7.11)

782

783 Here \mathcal{D} is an operator formed from $\partial \mathcal{L}^\dagger / \partial m$ by replacing each occurrence of δ with unity and
784 each occurrence of $\partial \delta / \partial x_i$ with $-\partial / \partial x_i$.

785 8. A Cross-Convolution Example Using the Elastic Wave Equation

786

787 8.1. The elastic Green function. In an isotropic and homogeneous solid, the far-field

788 displacement $u_{A,S}$ for an observer at \mathbf{x}_A and a point force in the $\hat{\mathbf{f}}$ direction at \mathbf{x}_S consists of the

789 sum of P-wave and S-wave terms (Aki and Richards 2009):

$$u_{A,S} = \frac{s(t - T_{S,A}^P)}{4\pi\rho\alpha^2 R_{A,S}} \hat{\mathbf{Y}}_{A,S} (\hat{\mathbf{Y}}_{A,S} \cdot \hat{\mathbf{f}}) + \frac{s(t - T_{S,A}^S)}{4\pi\rho\beta^2 R_{A,S}} \{\hat{\mathbf{f}} - \hat{\mathbf{Y}}_{A,S} (\hat{\mathbf{Y}}_{A,S} \cdot \hat{\mathbf{f}})\}$$

790 (8.1)

791

792 Here α and β are the compressional and shear wave velocities, respectively, ρ is density, $R_{S,A}$ is
 793 the distance from \mathbf{x}_A to \mathbf{x}_S , $T_{A,S}^P = R_{A,S} / \alpha$ is the travel time of the P wave, $T_{A,S}^S = R_{A,S} / \beta$ is the
 794 travel time of the S wave, $\hat{\mathbf{Y}}_{A,S} = (\mathbf{x}_A - \mathbf{x}_S) / R_{A,S}$ is the direction from source to observer, and
 795 $s(t)$ is the source time function.

796 We limit our discussion to P-S_v displacements from sources and receivers in the (x_1, x_3) plane.

797 A force in the x_1 -direction causes displacement:

$$\begin{bmatrix} u_x^0 \\ u_z^0 \end{bmatrix}_A = \frac{s(t - T_{A,S}^P)}{4\pi\rho\alpha^2 R_{A,S}} \begin{bmatrix} \cos^2 \theta_{S,A} \\ \sin \theta_{S,A} \cos \theta_{S,A} \end{bmatrix} + \frac{s(t - T_{A,S}^S)}{4\pi\rho\beta^2 R_{A,S}} \begin{bmatrix} \sin^2 \theta_{A,S} \\ -\sin \theta_{A,S} \cos \theta_{A,S} \end{bmatrix}$$

798 (8.2)

799 Here $\theta_{A,S}$ is the angle from the x_1 -direction to the observer. A force in the x_3 -direction causes
 800 displacement:

$$\begin{bmatrix} u_x^0 \\ u_z^0 \end{bmatrix}_A = \frac{s(t - T_{S,A}^P)}{4\pi\rho\alpha^2 R_{A,S}} \begin{bmatrix} \sin \theta_{S,A} \cos \theta_{A,S} \\ \sin^2 \theta_{A,S} \end{bmatrix} + \frac{s(t - T_{S,A}^S)}{4\pi\rho\beta^2 R_{A,S}} \begin{bmatrix} -\sin \theta_{A,S} \cos \theta_{A,S} \\ \cos^2 \theta_{A,S} \end{bmatrix}$$

801 (8.3)

802

803 In each case, the P and S wave particle motions are mutually perpendicular.

804 8.2. Derivatives of Power and Cross-Convolution Measure with Respect to Model Parameters.

805 We focus on the displacement field due to a force in the x_1 -direction, located at $\mathbf{x}_S = 0$ and with
806 a Gaussian source time function. The P wave observed at \mathbf{x}_R consists of a leading “direct” wave
807 followed by a secondary “scattered” wave. It is selected from the time series by multiplication
808 by the boxcar window function $\Omega(t)$. In the absence of heterogeneity, the predicted P wave
809 consists only of the direct wave. Heterogeneity leads to scattering, which results in scattered
810 waves, some of which may match the observed secondary arrival. We consider a sequence of
811 point density heterogeneities, each of strength m and located at a position \mathbf{x}_H . The derivative
812 $\partial\Phi/\partial m$ quantifies whether one or more of these heterogeneities can improve the fit.

813 We compute $\partial\Psi/\partial m$, $\partial P/\partial m$ and $\partial\Phi/\partial m$ for a grid of \mathbf{x}_H 's in the (x, y) plane using both the
814 direct and adjunct method:

815 The direct method computes the derivative by comparing windowed predicted and observed
816 waves at the position of the receiver. The predicted wave is the sum of a direct wave plus a
817 scattered wave. The former is calculated by forward-propagating P and S waves from the source
818 to the observer. The latter is calculated by forward-propagating P and S waves to the
819 heterogeneity, where they act as secondary sources that generate scattered P and S waves that are
820 then propagated to the receiver. The direct and scattered waves are summed and windowed
821 around the P wave arrival time to yield the predicted wave. It's power and cross-convolution
822 measure are calculated and compared with those of the direct wave, providing a finite difference
823 approximation of the derivatives.

824 The adjoint method computes the each derivative by comparing two time series at the position of
825 the heterogeneity. One time series is the second derivative of source forward-propagated to the

826 heterogeneity. The other is the adjoint wave field, which is back-propagated from an adjoint
827 source at the receiver to the heterogeneity. The two time series are the “correlated” by time-
828 integrating their product, yielding the derivative. Two different adjoint wave fields must be
829 calculated, one for $\partial\Psi/\partial m$ and the other for $\partial P/\partial m$ (Figure 5).

830 We have verified that these two methods produce the same result. In both cases, each of the four
831 scattering interactions (P→P, P→S, S→P and S→S) can be isolated simply by omitting a P or S
832 wave from each of the two stages of propagation.

833 8.3 Resolution. Resolving power is an important one for understanding the behavior and utility
834 of any inverse problem [Backus and Gilbert, 1968, 1971, Wiggins 1972, see also Menke 2014].
835 We first compute the wave field, observed at an array of receivers, associated with a point-like
836 heterogeneity in density at \mathbf{x}_H ; it becomes the synthetic data \mathbf{u}^{obs} . We then perform an
837 approximate inversion of these data to produce an estimate of the heterogeneity. Typically, the
838 heterogeneity spreads out in space, so it can be interpreted as a *point spread function* that
839 quantifies resolution.

840 Suppose that we define a gradient vector $[\nabla\Phi]_i \equiv \partial\Phi/\partial m_i$, each element of which corresponds
841 to the derivative for a point heterogeneity at $\mathbf{x}^{(i)}$ of amplitude m_i . The steepest-descent estimate
842 of these amplitudes is computed by moving a distance Δm , in the downhill direction, from the
843 homogeneous $\mathbf{m}^0 = 0$ model (corresponding to Φ_0) to a heterogeneous model \mathbf{m}^{est}
844 (corresponding to $\Phi \approx 0$):

$$0 - \Phi_0 \approx \nabla\Phi \cdot (\mathbf{m}^{est} - 0) \quad \text{with} \quad \mathbf{m}^{est} = \frac{\nabla\Phi}{|\nabla\Phi|} \Delta m$$

$$\phi_0 \approx -\nabla\phi \cdot \frac{\nabla\phi}{|\nabla\phi|} \Delta m \quad \text{so} \quad \Delta m = -\frac{\phi_0}{|\nabla\phi|} \quad \text{and} \quad \mathbf{m}^{\text{est}} \approx \frac{-\phi_0}{|\nabla\phi|^2} \nabla\phi$$

845 (8.4)

846 In this approximation, the solution \mathbf{m}^{est} is proportional to the gradient $\nabla\phi$, implying that $\nabla\phi$ can
847 be used as an proxy for the point spread function. We examine three cases, in which the window
848 function is chosen to include both P and S waves, or just the P wave, or just the S wave. In all
849 three cases, $\nabla\phi$ has sharp minimum at \mathbf{x}_H , implying a narrow point spread function and excellent
850 resolution (although the horizontal resolution in the P wave case is poorer than the other two
851 (Figure 6).

852 9. Conclusions

853 The Adjoint Methods have proven to be essential tools for imaging problems. On the practical
854 side, they allow inversions to be organized in an extremely efficient way, allowing what might
855 otherwise be prohibitively time-consuming calculations to be performed. On the conceptual side,
856 they allow complex formula to be manipulated into forms in which important quantities, such as
857 Fréchet derivatives, readily can be identified. Our review here has stressed the underlying
858 similarity between different approaches used in the literature, including the derivation of the
859 adjoint field equations, the use of partial or Fréchet derivatives, and the application of the
860 method to four different types of data (wave forms, finite frequency travel times, power and
861 cross-correlation measure).

862 Acknowledgements. This research was supported by the National Science Foundation under
863 grant EAR 11-47742.

864

865 References

866 Aki, K. and P.G. Richards, Quantitative Seismology, Second Edition, 700 pp, ISBN-13: 978-
867 1891389634, 2009.

868 Backus, G. and F. Gilbert, The resolving power of Gross Earth Data, Geophys. J.R. astr. Soc.16,
869 169-205, doi: 10.1190/1.1444834.coden:GPYSA70016-8033, 1968.

870 Backus G., and F. Gilbert., 1970, Uniqueness in the inversion of inaccurate gross earth data,
871 Philosophical Transactions of the Royal Society of London Series A, 266, 123–192, doi:
872 10.1098/rsta.1970.0005.coden:PTRMAD1364-503X, 1971.

873 Bodin, T., H. Yuan, and B. Romanowicz, Inversion of receiver functions without
874 deconvolution—application to the Indian craton, Geophys. J. Int., 196(2), 1025-1033,
875 doi:10.1093/gji/ggt431, 2014.

876 Chauhan, A.P.S., S. Singh, N.D. Hananto, H. Carton, F. Klingelhoefer, J.-X. Dessa, H. Permana,
877 N.J. White, D. Graindorge, and the SumatraOBS Scientific Team, Seismic imaging of forearc
878 backthrusts at northern Sumatra subduction zone, Geophys. J. Int. 179 : 1772-1780, doi:
879 10.1111/j.1365-246X.2009.04378.x, 2009.

880 Chen, P., L. Zhao and T.H. Jordan, Full 3D Tomography for Crustal Structure of the Los
881 Angeles Region, 2007, Bulletin of Seismological Society of America 97, 1094-1120, doi:
882 10.1785/0120060222, 2007.

883

884 Chen, P., T.H. Jordan and E.-J. Lee, Perturbation Kernels for Generalized Seismological Data
885 Functionals (GSDF), *Geophysical Journal International*, 183, 869-883, doi: 10.1111/j.1365-
886 246X.2010.04758.x, 2010.

887 Claerbout, J.F. and S.M. Doherty, Downward continuation of moveout-corrected seismograms,
888 *Geophysics*, 37, 741-768. doi: 10.1190/1.1440298, 1972.

889 Coppens, F., First arrival picking on common-offset trace collections for automatic estimation of
890 static corrections, *Geophysical Prospecting* 33, 1212-1231, DOI: 10.1111/j.1365-
891 2478.1985.tb01360, 1985.

892 Dahlen, F.A., S.-H. Hung and G. Nolet, Fréchet kernels for finite-frequency traveltimes—I.
893 Theory, *Geophys. J. Int.* 141, 157-174, doi: 10.1046/j.1365-246X.2000.00070.x, 2000.

894 Deuffhard, P., *Newton Methods for Nonlinear Problems. Affine Invariance and Adaptive*
895 *Algorithms. Springer Series in Computational Mathematics 35.* Springer, 424pp, ISBN 3-540-
896 21099-7, 2004.

897 Devaney, A.J., Inverse-scattering theory within the Rytov approximation. *Optics Letters* 6, 374-
898 376. doi: 10.1364/OL.6.000374, 1981.

899 Hall, M.C.G., D.C. Cacuci and M.E. Schlesinger, Sensitivity Analysis of a Radiative-Convective
900 Model by the Adjoint Method, *J. Atmospheric Sci.* 39, 2038-2050, DOI: 10.1175/1520-
901 0469(1982)039<2038:SAOARC>2.0.CO;2, 1982.

902 Hall, M.C.G. and D.G. Cacuci, Physical interpretation of the adjoint functions for sensitivity
903 analysis of atmospheric models. *J. Atmos. Sci.* 40, 2537–2546, doi: 10.1175/1520-
904 0469(1983)040<2537:PIOTAF>2.0.CO;2, 1983.

905 Hung, S.-H., F.A. Dahlen and G. Nolet, Fréchet kernels for finite-frequency traveltimes—II.
906 Examples, *Geophys. J. Int.* 141, 175-203, doi: 10.1046/j.1365-246X.2000.00072.x, 2000.

907 Kim, Y., Liu, Q., and J. Tromp. Adjoint centroid-moment tensor inversions. *Geophys. J. Int.*,
908 186: 264-278. DOI: 10.1111/j.1365-246X.2011.05027.x, 2011.

909 Long, M.D., M. de Hoop and R.D. van der Hilst, Wave-equation shear wave splitting
910 tomography, *Geophys. J. Int.*, 172, 311-330, DOI: 10.1111/j.1365-246X.2007.03632.x, 2008

911 Luo, Y., Tromp, J., Denel, B., and Calendra, H. 3D coupled acoustic-elastic migration with
912 topography and bathymetry based on spectral-element and adjoint methods. *Geophysics* 78,
913 S193-S202. doi: 10.1190/geo2012-0462.1, 2013.

914 Marquering, H., G. Nolet G. and F.A. Dahlen, Three-dimensional waveform sensitivity kernels,
915 *Geophys. J. Int.* 132, 521–534, DOI: 10.1046/j.1365-246X.1998.00426.x, 1998.

916 Marquering, H, FA Dahlen, G. Nolet, Three-dimensional sensitivity kernels for finite-frequency
917 traveltimes: the banana-doughnut paradox, *Geophys. J. Int.* 137, 805-815. doi: 10.1046/j.1365-
918 246x.1999.00837.x, 1999.

919 Mellman, G.R., A method of body-wave waveform inversion for the determination of earth
920 structure, *Geophys. J. Int.* 62, 481-504. doi: 10.1111/j.1365-246X.1980.tb02587.x, 1980.

921 Menke, W. *Geophysical Data Analysis: Discrete Inverse Theory, Third Edition (textbook)*,
922 Academic Press (Elsevier), 330 pp, ISBN: 9780123971609, 2012.

923 Menke, W., Review of the Generalized Least Squares Method, *Surveys in Geophysics* 36, 1-25,
924 doi: 10.1007/s10712-014-9303-1, 2014.

925 Menke, W. and Z. Eilon, Relationship between data smoothing and the regularization of inverse
926 problems, *Pure and Applied Geophysics* 172, 2711-2726, DOI: 10.1007/s00024-015-1059-0,
927 2015

928 Menke, W. and V. Levin, The cross-convolution method for interpreting SKS splitting
929 observations, with application to one and two-layer anisotropic earth models, *Geophys. J. Int.*
930 154, 379-392, doi: 10.1046/j.1365-246X.2003.01937.x, 2003.

931

932 Montelli, R., G. Nolet, F.A. Dahlen and G. Masters, Finite-frequency tomography
933 reveals a variety of plumes in the mantle, *Science* 303, 338-343, DOI: 10.1126/science.1092485,
934 2006.

935

936 Reed, M. and S. Barry, *Functional Analysis*, Elsevier, 400 pp, ISBN 0125850506, 1981.

937

938 Snyman, J.A., *Practical Mathematical Optimization: An Introduction to Basic Optimization*
939 *Theory and Classical and New Gradient-Based Algorithms*, Springer Publishing, 257 pp, ISBN
940 0-387-24348-8, 2005.

941

942 Talagrand, O. and P. Courtier, Variational Assimilation of Meteorological Observations with the
943 Adjoint Vorticity Equation. I: Theory, *Quarterly Journal of the Royal Meteorological Society*
944 113, 1311–1328 DOI: 10.1002/qj.49711347812, 1987.

945

946 Taillandier, C. M. Noble, H. Chauris and H. Calandra, First-arrival traveltime tomography based
947 on the adjoint-state method, *Geophysics* 74, WCB1–WCB10, doi: 10.1190/1.3250266, 2009.

948

949 Tromp, J., C. Tape and Q. Liu, Seismic Tomography, adjoint methods, time reversal and banana-
950 doughnut kernels, *Geophys. J. Int.* 160, 195-216, doi: 10.1111/j.1365-246X.2004.02453.x, 2005.

951

952 van der Hilst, R.D., and M.V. De Hoop, Banana-doughnut kernels and mantle tomography,
953 *Geophys. J. Int.* 163, 956-961, doi: 10.1111/j.1365-246X.2005.02817.x, 2005.

954

955 Wiggins, R.A., The general linear inverse problem: Implications of surface waves and free
956 oscillations for Earth structure, *Rev. Geophys. Space Phys.* 10, 251-285, doi:
957 10.1029/RG010i001p00251, 1972.

958

959 Xu, Z., P. Chen and Y. Chen, Sensitivity Kernel for the Weighted Norm of the Frequency-
960 Dependent Phase Correlation, *Pure and Applied Geophysics* 170, 353-371, DOI 10.1007/s00024-
961 012-0507-3, 2012.

962

963 Zhao, L. T.H. Jordan, KB. Olsen and P. Chen, Fréchet Kernels for Imaging Regional Earth
964 Structure Based on Three-dimensional Reference Models, *Bulletin of Seismological Society of*
965 *America* 95, 2066-2080, doi: 10.1785/0120050081, 2005.

966

967 Zhu, H., E. Bozdag, D. Peter, and J. Tromp. Structure of the European upper mantle revealed by
968 adjoint tomography. *Nature Geoscience* 5, 493-498, doi: 10.1038/ngeo1501, 2012.

969

970 Zhu, H., Y. Luo, T. Nissen-Meyer, C. Morency and J. Tromp, Elastic imaging and time-lapse
 971 migration based on adjoint methods, *Geophysics* 74, WCA167-WCA177, doi:
 972 10.1190/1.3261747, 2009.

973 .Appendix

974 A.1. Adjoint of Some Simple Operators. A function $f(\mathbf{x}, t)$ is self-adjoint, since:

$$\begin{aligned} \langle fu, v \rangle &= \int_t \iiint_{\mathbf{x}} \{f(\mathbf{x}, t) u(\mathbf{x}, t)\} v(\mathbf{x}, t) d^3\mathbf{x} dt \\ &= \int_t \iiint_{\mathbf{x}} u(\mathbf{x}, t) \{f(\mathbf{x}, t) v(\mathbf{x}, t)\} d^3\mathbf{x} dt = \langle u, fv \rangle \end{aligned}$$

975 (A.1)

976

977 The first derivative $\partial/\partial t$ is anti-self-adjoint, since by integration by parts:

$$\langle \frac{\partial u}{\partial t}, v \rangle = \int_t \iiint_{\mathbf{x}} \left\{ \frac{\partial}{\partial t} u(\mathbf{x}, t) \right\} v(\mathbf{x}, t) d^3\mathbf{x} dt = \iiint_{\mathbf{x}} \int_{t_{min}}^{t_{max}} \left\{ \frac{\partial}{\partial t} u(\mathbf{x}, t) \right\} v(\mathbf{x}, t) dt d^3\mathbf{x}$$

978

$$= \iiint_{\mathbf{x}} \int_t \{u(\mathbf{x}, t) v(\mathbf{x}, t)\} \Big|_{t_{min}}^{t_{max}} dt d^3\mathbf{x} - \iiint_{\mathbf{x}} \int_t u(\mathbf{x}, t) \left\{ \frac{\partial}{\partial t} v(\mathbf{x}, t) \right\} dt d^3\mathbf{x} = \langle u, -\frac{\partial v}{\partial t} \rangle$$

979 (A.2)

980

981 (provided that the fields decline to zero at $t \rightarrow \pm\infty$). The second derivative $\partial^2/\partial t^2$ is self-

982 adjoint, since:

$$\left(\frac{\partial^2}{\partial t^2}\right)^\dagger = \left(\frac{\partial}{\partial t} \frac{\partial}{\partial t}\right)^\dagger = \left(\frac{\partial}{\partial t}\right)^\dagger \left(\frac{\partial}{\partial t}\right)^\dagger = \left(-\frac{\partial}{\partial t}\right) \left(-\frac{\partial}{\partial t}\right) = \frac{\partial^2}{\partial t^2}$$

983 (A.3)

984

985 The adjoint of a Green function inner product obeys:

986

$$\text{If } \mathcal{G}_A y_A = \langle G_{A,B}, y_B \rangle_B \text{ then } \mathcal{G}_A^\dagger y_A = \langle G_{B,A}^\dagger, y_B \rangle_B$$

987 (A.4)

988

989 since

$$\begin{aligned} \langle \mathcal{G}_A y_A, z_A \rangle_A &= \langle \langle G_{A,B} y_B \rangle_B, z_A \rangle_A = \langle \langle G_{A,B} y_B, z_A \rangle_A \rangle_B \\ &= \langle y_B, \langle G_{A,B}^\dagger z_A \rangle_A \rangle_B = \langle y_B, \mathcal{G}_B^\dagger z_B \rangle_B \end{aligned}$$

990 (A.5)

991

992 The adjoint of a convolution is a cross-correlation:

$$\begin{aligned} \langle a * u, v \rangle &= \int_t \iiint_{\mathbf{x}} \int_{\tau} a(\tau) u(t - \tau) d\tau v(t) d^3\mathbf{x} dt \\ &= \int_{\tau'} \iiint_{\mathbf{x}} u(\tau') \int_{\tau} a(\tau) v(\tau + \tau') d\tau d^3\mathbf{x} d\tau' = \langle u, a * v \rangle \end{aligned}$$

993 (A.6)

994

995 Here we have employed the transformation $\tau' = t - \tau$.

996 The adjoint of a matrix operator is the transposed matrix of adjoints:

$$\begin{aligned}
 & \left\langle \begin{bmatrix} \mathcal{L}_{11} & \mathcal{L}_{12} \\ \mathcal{L}_{21} & \mathcal{L}_{22} \end{bmatrix} \begin{bmatrix} a_1 \\ a_2 \end{bmatrix}, \begin{bmatrix} b_1 \\ b_2 \end{bmatrix} \right\rangle = \left\langle \begin{bmatrix} \mathcal{L}_{11}a_1 + \mathcal{L}_{12}a_2 \\ \mathcal{L}_{21}a_1 + \mathcal{L}_{22}a_2 \end{bmatrix}^T \begin{bmatrix} b_1 \\ b_2 \end{bmatrix} \right\rangle \\
 & = \langle \mathcal{L}_{11}a_1, b_1 \rangle + \langle \mathcal{L}_{12}a_2, b_1 \rangle + \langle \mathcal{L}_{21}a_1, b_2 \rangle + \langle \mathcal{L}_{22}a_2, b_2 \rangle \\
 & = \langle a_1, \mathcal{L}_{11}^\dagger b_1 \rangle + \langle a_2, \mathcal{L}_{12}^\dagger b_1 \rangle + \langle a_1, \mathcal{L}_{21}^\dagger b_2 \rangle + \langle a_2, \mathcal{L}_{22}^\dagger b_2 \rangle \\
 & = \left\langle \begin{bmatrix} a_1 \\ a_2 \end{bmatrix}^T \begin{bmatrix} \mathcal{L}_{11}^\dagger b_1 + \mathcal{L}_{21}^\dagger b_2 \\ \mathcal{L}_{12}^\dagger b_1 + \mathcal{L}_{22}^\dagger b_2 \end{bmatrix} \right\rangle = \left\langle \begin{bmatrix} a_1 \\ a_2 \end{bmatrix}, \begin{bmatrix} \mathcal{L}_{11}^\dagger & \mathcal{L}_{12}^\dagger \\ \mathcal{L}_{21}^\dagger & \mathcal{L}_{22}^\dagger \end{bmatrix}^T \begin{bmatrix} b_1 \\ b_2 \end{bmatrix} \right\rangle
 \end{aligned}$$

997

(A.7)

998

999 The operator \mathcal{L} of the elastic wave equation is self-adjoint. Each diagonal element is self-adjoint;

1000 for instance, the (1,1) element:

$$\left(\rho \frac{\partial^2}{\partial t^2} - (\lambda + 2\mu) \frac{\partial^2}{\partial x^2} - \mu \frac{\partial^2}{\partial y^2} - \mu \frac{\partial^2}{\partial z^2} - \frac{\partial(\lambda + 2\mu)}{\partial x} \frac{\partial}{\partial x} - \frac{\partial\mu}{\partial y} \frac{\partial}{\partial y} - \frac{\partial\mu}{\partial z} \frac{\partial}{\partial z} \right)^\dagger =$$

1001

$$\begin{aligned}
 & \left(\rho \frac{\partial^2}{\partial t^2} - \frac{\partial}{\partial x} (\lambda + 2\mu) \frac{\partial}{\partial x} - \frac{\partial}{\partial y} \mu \frac{\partial}{\partial y} - \frac{\partial}{\partial z} \mu \frac{\partial}{\partial z} \right)^\dagger \\
 & = \rho \frac{\partial^2}{\partial t^2} - \frac{\partial}{\partial x} (\lambda + 2\mu) \frac{\partial}{\partial x} - \frac{\partial}{\partial y} \mu \frac{\partial}{\partial y} - \frac{\partial}{\partial z} \mu \frac{\partial}{\partial z}
 \end{aligned}$$

1002

(A.8)

1003

1004

1005 And each pair off diagonal elements are adjoints of one another; for instance for the (1,2) and

1006 (2,1) pair:

1007

$$\left(-(\lambda + \mu) \frac{\partial^2}{\partial x \partial y} - \frac{\partial \lambda}{\partial x} \frac{\partial}{\partial y} - \frac{\partial \mu}{\partial y} \frac{\partial}{\partial x} \right)^\dagger = \left(-\frac{\partial}{\partial x} \lambda \frac{\partial}{\partial y} - \frac{\partial}{\partial y} \mu \frac{\partial}{\partial x} \right)^\dagger = -\frac{\partial}{\partial y} \lambda \frac{\partial}{\partial x} - \frac{\partial}{\partial x} \mu \frac{\partial}{\partial y}$$

1008

$$-(\lambda + \mu) \frac{\partial^2}{\partial x \partial z} - \frac{\partial \lambda}{\partial y} \frac{\partial}{\partial x} - \frac{\partial \mu}{\partial x} \frac{\partial}{\partial y} = -\frac{\partial}{\partial y} \lambda \frac{\partial}{\partial x} - \frac{\partial}{\partial x} \mu \frac{\partial}{\partial y}$$

1009

(A.9)

1010 An adjoint can have different boundary conditions than the original operator. Consider the first

1011 derivative du/dt with the initial condition $u(t = 0) = 0$, written as the operator $\mathcal{L}u$. It has a

1012 finite difference approximation $\mathbf{L}\mathbf{u}$, where:

$$\mathcal{L} \approx \mathbf{L} = \begin{bmatrix} -1 & 0 & 0 & 0 \\ 1 & -1 & 0 & 0 \\ 0 & 1 & -1 & 0 \\ 0 & 0 & 1 & -1 \end{bmatrix}$$

1013

(A.10)

1014

1015 The first row of $\mathbf{L}\mathbf{u}$ involves only the first element of \mathbf{u} and is the initial condition; the

1016 subsequent rows are the first differences between adjacent elements of \mathbf{u} and is the derivative.

1017 The corresponding approximation of operator \mathcal{L}^\dagger is the transposed matrix:

$$\mathcal{L}^\dagger \approx \mathbf{L}^T = \begin{bmatrix} -1 & 1 & 0 & 0 \\ 0 & -1 & 1 & 0 \\ 0 & 0 & -1 & 1 \\ 0 & 0 & 0 & -1 \end{bmatrix}$$

1018 (A.11)

1019 Then boundary condition has moved to the last row of $\mathbf{L}^T \mathbf{u}$ has become an end condition and, as
 1020 expected, the signs of the first differences have flipped.

1021 A. 2. Derivative of the Inverse of an Operator. Perturbation theory can be used to show that, for
 1022 a small number ε , the inverse of $\mathcal{L}_0 + \varepsilon \mathcal{L}_1$ is [Menke and Eilon, 2015]:

$$[\mathcal{L}_0 + \varepsilon \mathcal{L}_1]^{-1} = \mathcal{L}_0^{-1} - \varepsilon \mathcal{L}_0^{-1} \mathcal{L}_1 \mathcal{L}_0^{-1} + O(\varepsilon^2)$$

1023 (A.12)

1024 This expression is verified by showing that applying the operator to its inverse, and the inverse to
 1025 the operator, both yield the identity operator \mathcal{I} :

$$[\mathcal{L}_0 + \varepsilon \mathcal{L}_1][\mathcal{L}_0^{-1} - \varepsilon \mathcal{L}_0^{-1} \mathcal{L}_1 \mathcal{L}_0^{-1} + O(\varepsilon^2)] = \mathcal{I} + \varepsilon[\mathcal{L}_1 \mathcal{L}_0^{-1} - \mathcal{L}_1 \mathcal{L}_0^{-1}] + O(\varepsilon^2) = \mathcal{I} + O(\varepsilon^2)$$

1026 and

$$[\mathcal{L}_0^{-1} - \varepsilon \mathcal{L}_0^{-1} \mathcal{L}_1 \mathcal{L}_0^{-1} + O(\varepsilon^2)][\mathcal{L}_0 + \varepsilon \mathcal{L}_1] = \mathcal{I} + \varepsilon[\mathcal{L}_0^{-1} \mathcal{L}_1 - \mathcal{L}_0^{-1} \mathcal{L}_1] + O(\varepsilon^2) = \mathcal{I} + O(\varepsilon^2)$$

1027 (A.13)

1028 The derivative rule then follows from the definition of the derivative:

$$\frac{\partial}{\partial m} \mathcal{L}^{-1} = \lim_{\Delta m \rightarrow 0} \frac{[\mathcal{L} + \left[\frac{\partial \mathcal{L}}{\partial m} \right] \Delta m]^{-1} - \mathcal{L}^{-1}}{\Delta m} = -\mathcal{L}^{-1} \left[\frac{\partial \mathcal{L}}{\partial m} \right] \mathcal{L}^{-1}$$

1029 (A.14)

1030 A.3. The Adjoint Field as a Lagrange Multiplier. For clarity, we derive the derivative $\partial E / \partial m$
 1031 (Equation 3.2) in the discrete case where the field $\mathbf{u}(\mathbf{x}, t)$ is approximated by a discrete vector u_i
 1032 with $i = 1, 2, \dots, K$ that contains $\mathbf{u}(\mathbf{x}, t)$ evaluated all permutations of components, positions and

1033 times. We consider a $(K + 1)$ -dimensional vector space consisting of the elements of the field
 1034 plus a single model parameter m (Figure A1). In this view, the elements of the field and the
 1035 model parameter are all independent variables. Using Einstein notation, where repeated indices
 1036 imply summation, the total error is $E = e_i e_i$ with $e_i = u_i^{obs} - u_i$. The error is independent of m ,
 1037 and is axially-symmetric about the line $u_i = u_i^{obs}$ (cylinder in Figure A1). The field obeys a
 1038 matrix equation $C_i \equiv L_{ij}(m) u_j - f_j = 0$, where the $K \times K$ matrix $\mathbf{L}(m)$ is a discrete analogue of
 1039 a differential operator $\mathcal{L}(m)$ and its associated boundary conditions. The use of the abbreviation
 1040 C_i highlights the sense in which each row of the matrix equation is a separate constraint applied
 1041 at a different point in space and time. Since, for any given value of m , the matrix equation can be
 1042 solved for a unique field $u_i(m)$, but the value of m can be freely varied, these constraint trace
 1043 out a curve (grey line in Figure A.1). We want to know the gradient of the error resolved onto
 1044 this curve, a quantity that we will refer to as $\partial E / \partial m|_{C=0}$.

1045 The explicit calculation of $\partial E / \partial m|_{C=0}$ in Section 3.2 starts with:

$$\frac{\partial E}{\partial m} = 2e_i \frac{\partial e_i}{\partial m} = -2e_i \frac{\partial u_i}{\partial m} = -2\mathbf{e}^T \frac{\partial \mathbf{u}}{\partial m}$$

1046 (A.15)

1047 and substitutes in the solution $\mathbf{u} = \mathbf{L}^{-1}\mathbf{f}$. The error is then an explicit function of the model
 1048 parameter and can be differentiated with respect to it:

$$\begin{aligned} \frac{\partial E}{\partial m} \Big|_{C=0} &= -2\mathbf{e}^T \frac{\partial}{\partial m} (\mathbf{L}^{-1}\mathbf{f}) = -2\mathbf{e}^T \frac{\partial \mathbf{L}^{-1}}{\partial m} \mathbf{f} = 2\mathbf{e}^T \mathbf{L}^{-1} \frac{\partial \mathbf{L}}{\partial m} \mathbf{L}^{-1}\mathbf{f} \\ &= 2\mathbf{e}^T \mathbf{L}^{-1} \frac{\partial \mathbf{L}}{\partial m} \mathbf{u} = 2 \left(\frac{\partial \mathbf{L}^T}{\partial m} \mathbf{L}^{-1T} \mathbf{e} \right)^T \mathbf{u} \end{aligned}$$

1049 (A.16)

1050 Note that we have used the fact that \mathbf{f} is not a function of m and have applied the rule

1051 $\partial \mathbf{L}^{-1} / \partial m = -\mathbf{L}^{-1} (\partial \mathbf{L} / \partial m) \mathbf{L}^{-1}$. Defining the adjoint field to be $\boldsymbol{\lambda} = \mathbf{L}^{-1T} \mathbf{e}$ leads to equations:

$$\left. \frac{\partial E}{\partial m} \right|_{\mathbf{c}=0} = 2 \left(\frac{\partial \mathbf{L}^T}{\partial m} \boldsymbol{\lambda} \right)^T \mathbf{u} \quad \text{and} \quad \mathbf{L}^T \boldsymbol{\lambda} = \mathbf{e}$$

1052 (A.17)

1053 We obtain the continuous limit by replacing vectors with functions, matrices with operators and

1054 the dot product with the inner product:

$$\left. \frac{\partial E}{\partial m} \right|_{\mathbf{c}=0} = 2 \left\langle \frac{\partial \mathcal{L}^\dagger}{\partial m} \lambda, u \right\rangle \quad \text{and} \quad \mathcal{L}^\dagger \lambda = \mathbf{e}$$

1055 (A.18)

1056 These expressions are the same as those derived previously in Equation 3.2.

1057 The same result can be achieved *implicitly*, using the method of Lagrange multipliers. We focus

1058 on a point m_0 along the curve $C_i = 0$. The derivative resolved onto the curve is the part of ∇E

1059 that is parallel to the curve; or equivalently, the part of ∇E that is *perpendicular* to the gradients

1060 ∇C_i of all of the constraints.

1061 The standard way of removing the part of ∇E that is parallel to ∇C_i is to subtract from ∇E just

1062 the right amount of each ∇C_i . We start by writing:

$$\nabla E|_{\mathbf{c}=0} = \nabla E + 2 \nabla C_i \lambda_i$$

1063 (A.19)

1064 where λ_i are a set of unknown coefficients (called *Lagrange multipliers*) and the factor of 2 has
 1065 been added to simplify the subsequent derivation. The coefficients are determined by the
 1066 conditions that $\nabla E|_{\mathbf{c}=0}$ is perpendicular to ∇C_i :

$$\nabla C_i \cdot \nabla E|_{\mathbf{c}=0} = 0$$

1067 (A.20)

1068 Various derivatives are needed to perform this dot product:

$$\frac{\partial E}{\partial u_k} = 2e_i \frac{\partial e_i}{\partial u_k} = -2e_i \frac{\partial u_i}{\partial u_k} = -2e_i \delta_{ik} = -2e_k \quad \text{so} \quad \nabla_{\mathbf{u}} E = -2\mathbf{e}$$

$$\frac{\partial E}{\partial m} = 0 \quad \text{so} \quad \nabla_{\mathbf{m}} E = 0$$

$$\frac{\partial C_i}{\partial u_k} = \frac{\partial}{\partial u_k} (L_{ij} u_j - f_j) = L_{ij} \frac{\partial u_j}{\partial u_k} = L_{ij} \delta_{ik} = L_{ik} \quad \text{so} \quad \nabla_{\mathbf{u}} C_i = \mathbf{L}$$

$$\frac{\partial C_i}{\partial m} = \frac{\partial}{\partial m} (L_{ij} u_j - f_j) = \frac{\partial L_{ij}}{\partial m} u_j \quad \text{so} \quad \nabla_{\mathbf{m}} C_i = \frac{\partial \mathbf{L}}{\partial m} \mathbf{u}$$

1069 (A.21)

1070 Defining $[\boldsymbol{\lambda}]_i \equiv \lambda_i$, $\nabla E \equiv [\nabla_{\mathbf{u}} E, \nabla_{\mathbf{m}} E]^T$ and $\nabla C_i \equiv [\nabla_{\mathbf{u}} C_i, \nabla_{\mathbf{m}} C_i]^T$ we have:

$$\begin{bmatrix} \nabla_{\mathbf{u}} E|_{\mathbf{c}=0} \\ \frac{\partial E}{\partial m}|_{\mathbf{c}=0} \end{bmatrix} = \nabla E + 2\lambda_i \nabla C_i = \begin{bmatrix} -2\mathbf{e} \\ 0 \end{bmatrix} + 2 \begin{bmatrix} \mathbf{L}^T \boldsymbol{\lambda} \\ \boldsymbol{\lambda}^T \frac{\partial \mathbf{L}}{\partial m} \mathbf{u} \end{bmatrix}$$

1071 (A.22)

1072 The coefficients $\boldsymbol{\lambda}$ are determined by that condition that the dot product $\nabla C_i \cdot \nabla E|_{\mathbf{c}=0}$ is zero:

$$\mathbf{L}(\mathbf{e} - \mathbf{L}^T \boldsymbol{\lambda}) + \mathbf{u}^T \frac{\partial \mathbf{L}^T}{\partial m} \boldsymbol{\lambda}^T \frac{\partial \mathbf{L}}{\partial m} \mathbf{u} = 0$$

1073 (A.23)

1074 The choice

$$\mathbf{L}^T \boldsymbol{\lambda} = \mathbf{e}$$

1075 (A.24)

1076 zeros the first term on the l.h.s. It also zeros the second term, since:

$$\begin{aligned} \mathbf{u}^T \frac{\partial \mathbf{L}^T}{\partial m} \boldsymbol{\lambda}^T \frac{\partial \mathbf{L}}{\partial m} \mathbf{u} &= \mathbf{u}^T \frac{\partial \mathbf{L}^T}{\partial m} \mathbf{e}^T \mathbf{L}^{-1} \frac{\partial \mathbf{L}}{\partial m} \mathbf{L}^{-1} \mathbf{f} = -\mathbf{u}^T \frac{\partial \mathbf{L}^T}{\partial m} \mathbf{e}^T \frac{\partial \mathbf{L}^{-1}}{\partial m} \mathbf{f} \\ &= -\mathbf{u}^T \frac{\partial \mathbf{L}^T}{\partial m} \mathbf{e}^T \frac{\partial}{\partial m} (\mathbf{L}^{-1} \mathbf{f}) = -\mathbf{u}^T \frac{\partial \mathbf{L}^T}{\partial m} \mathbf{e}^T \frac{\partial \mathbf{u}}{\partial m} = 0 \end{aligned}$$

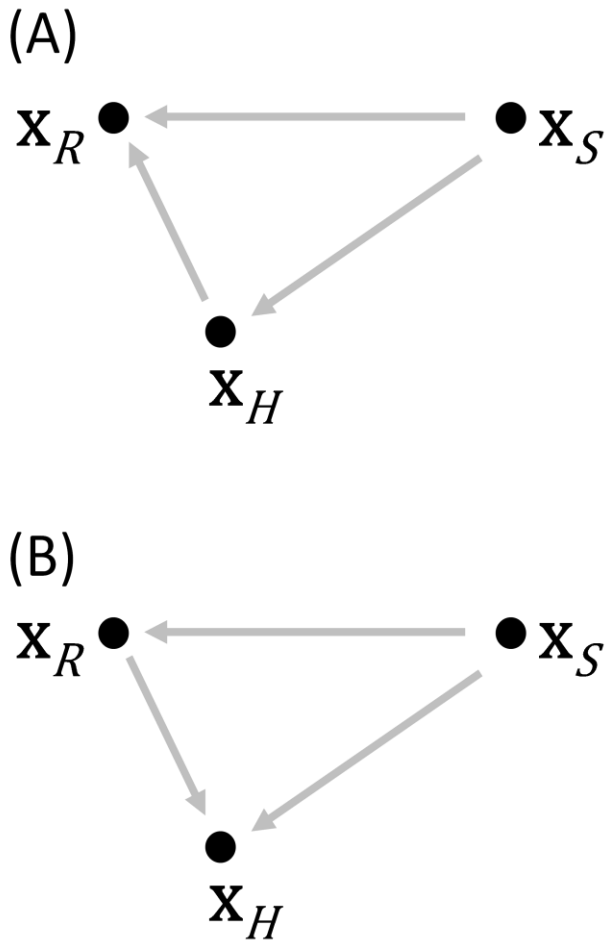
1077 (A.25)

1078 Here we have used the rules $\boldsymbol{\lambda}^T = \mathbf{e}^T \mathbf{L}^{-1}$, $\mathbf{u} = \mathbf{L}^{-1} \mathbf{f}$ and $\partial \mathbf{L}^{-1} / \partial m = \mathbf{L}^{-1} (\partial \mathbf{L} / \partial m) \mathbf{L}^{-1}$. The
 1079 derivative $\partial \mathbf{u} / \partial m$ is zero because, in the context of this derivation, \mathbf{u} and m are independent
 1080 variables. The lower part of Equation (A.20) gives:

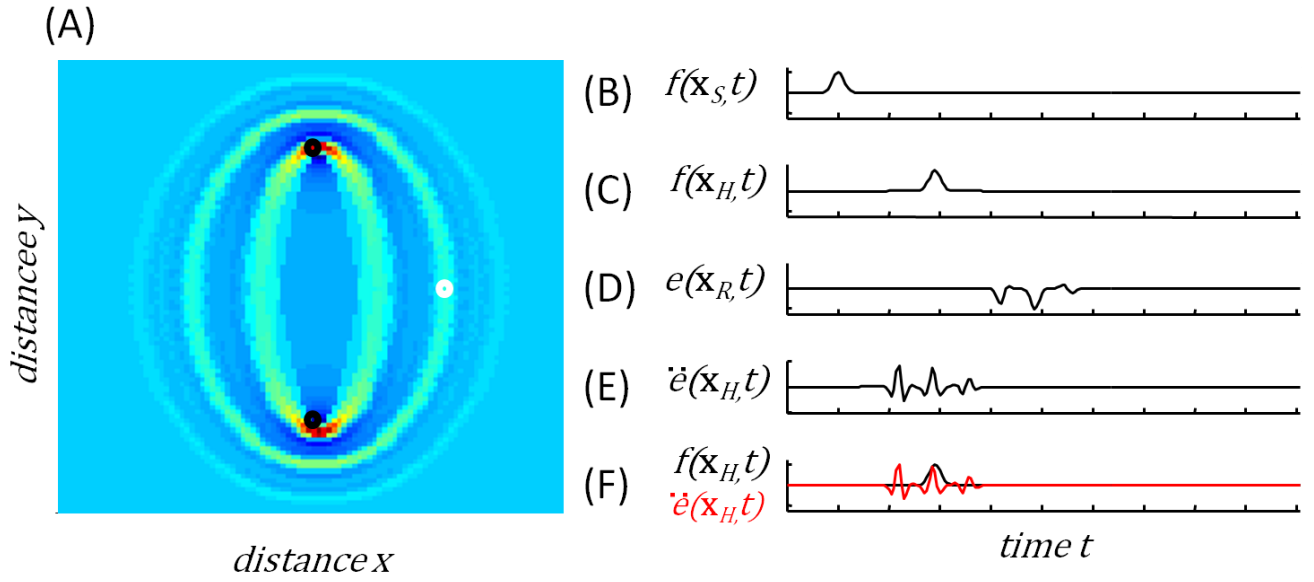
$$\left. \frac{\partial E}{\partial m} \right|_{\mathbf{c}=0} = 2 \left(\frac{\partial \mathbf{L}}{\partial m} \mathbf{u} \right)^T \boldsymbol{\lambda} = 2 \left(\frac{\partial \mathbf{L}^T}{\partial m} \boldsymbol{\lambda} \right)^T \mathbf{u}$$

1081 (A.26)

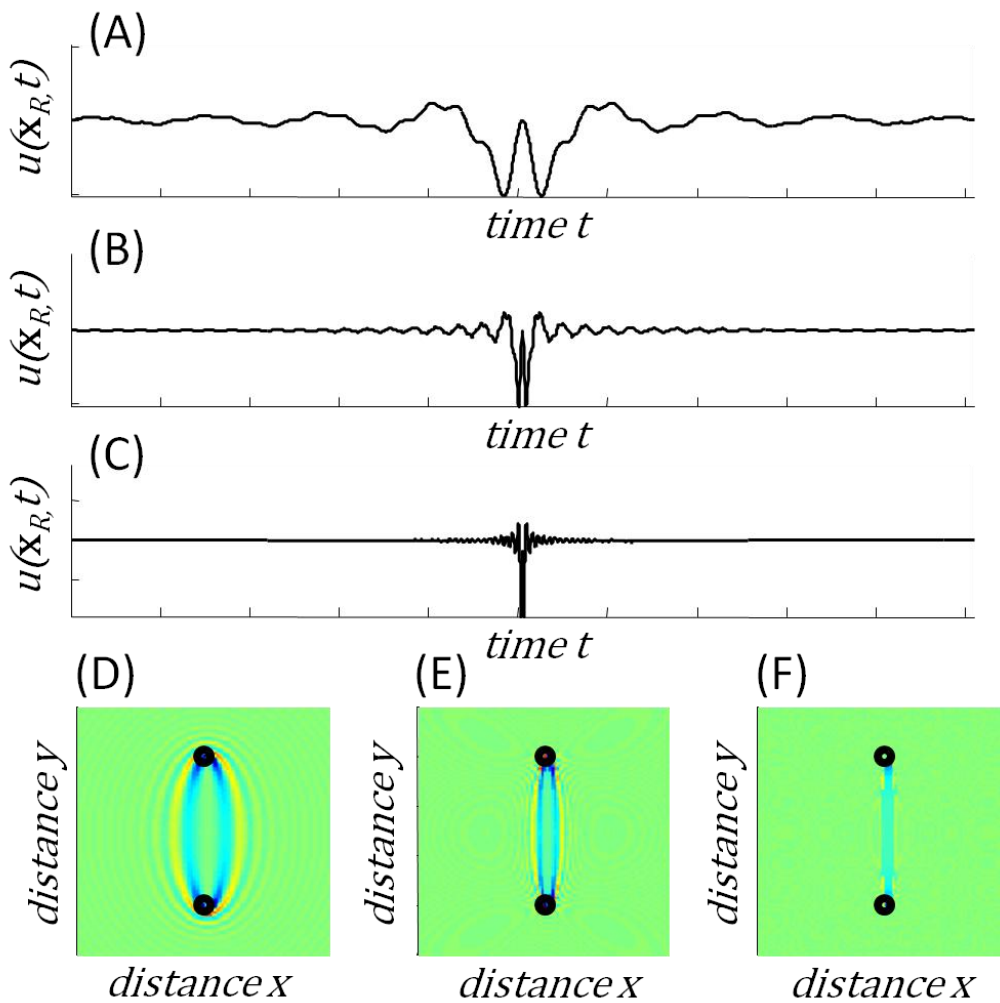
1082 This equation and Equation (A.14) are precisely the same as those derived by the explicit
 1083 method. Thus the Adjoint field $\boldsymbol{\lambda}$ can be interpreted as a Lagrange multiplier that arises from the
 1084 constraint that the field exactly satisfies a differential equation at every point in space and time.



1088 Fig. 1. (A) The Direct Method focuses on the two fields incident upon a receiver at \mathbf{x}_R : direct
1089 wave from the source at \mathbf{x}_S that follows the SR path; and a scattered wave that has interacted
1090 with a heterogeneity at \mathbf{x}_H and follows the SHR path. (B) The Adjoint Method focuses upon the
1091 fields incident upon the heterogeneity at \mathbf{x}_H , which includes the direct wave that follows the SH
1092 path and the adjoint field that follows the RH path. The source of the adjoint field depends upon
1093 the direct wave at the receiver, which follows the SR path.



1101 Figure 2. (A) The partial derivative $\partial E/\partial m$ (colors) for a point slowness heterogeneity in a
 1102 homogeneous acoustic whole space. The amplitude of the derivatives track ellipses of equal
 1103 travel time from source (lower black circle) to heterogeneity to receiver (upper black circle). (B)
 1104 The source time function $f(\mathbf{x}_S, t)$. (C) The source time function $f(\mathbf{x}_H, t)$ time-shifted to the
 1105 receiver at \mathbf{x}_R . (D) The error $e(\mathbf{x}_R, t)$ at the receiver. (E) The second derivative $\ddot{e}(\mathbf{x}_H, t)$, time-
 1106 shifted to a heterogeneity at \mathbf{x}_H (white circle in Part A). (F) Comparison $\ddot{e}(\mathbf{x}_H, t)$, (red
 1107 curve) and $f(\mathbf{x}_H, t)$. The overall in high-amplitudes leads to one of the elliptical bands in Part A.



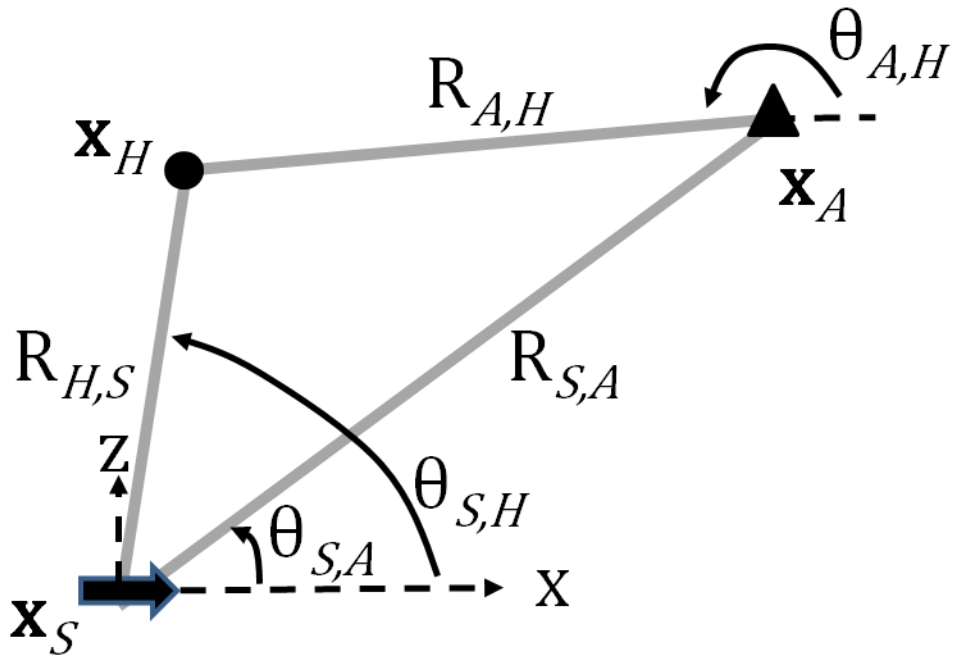
1109

1110

1111 Fig. 3. Quantities associated with the banana-doughnut kernel $\partial\tau/\partial m$. (A)-(C). Three band-
 1112 limited pulses $u^0(\mathbf{x}_R, t)$ originating from a source at \mathbf{x}_R and observed at a receiver at \mathbf{x}_R . The
 1113 peak frequency of these fields increases from A to C. (D)-(F) Banana-doughnut kernels (colors)
 1114 for point slowness homogeneities distributed on the (x, y) plane corresponding to the pulses in
 1115 Parts A-C. Note that the kernels narrow and become more linear with increasing frequency, as
 1116 diffraction behavior become less importance and ray-like behavior begins to dominate.

1117 Menke, Figure 4.

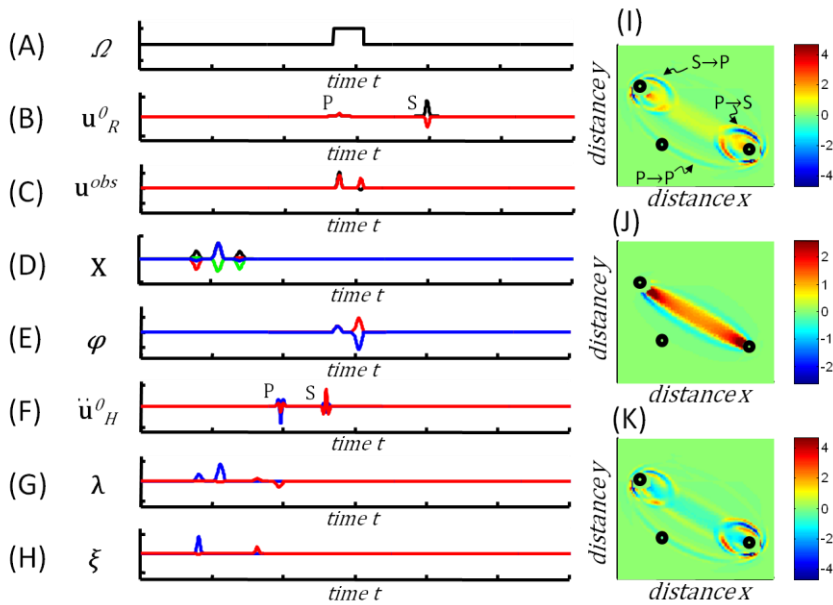
1118



1119

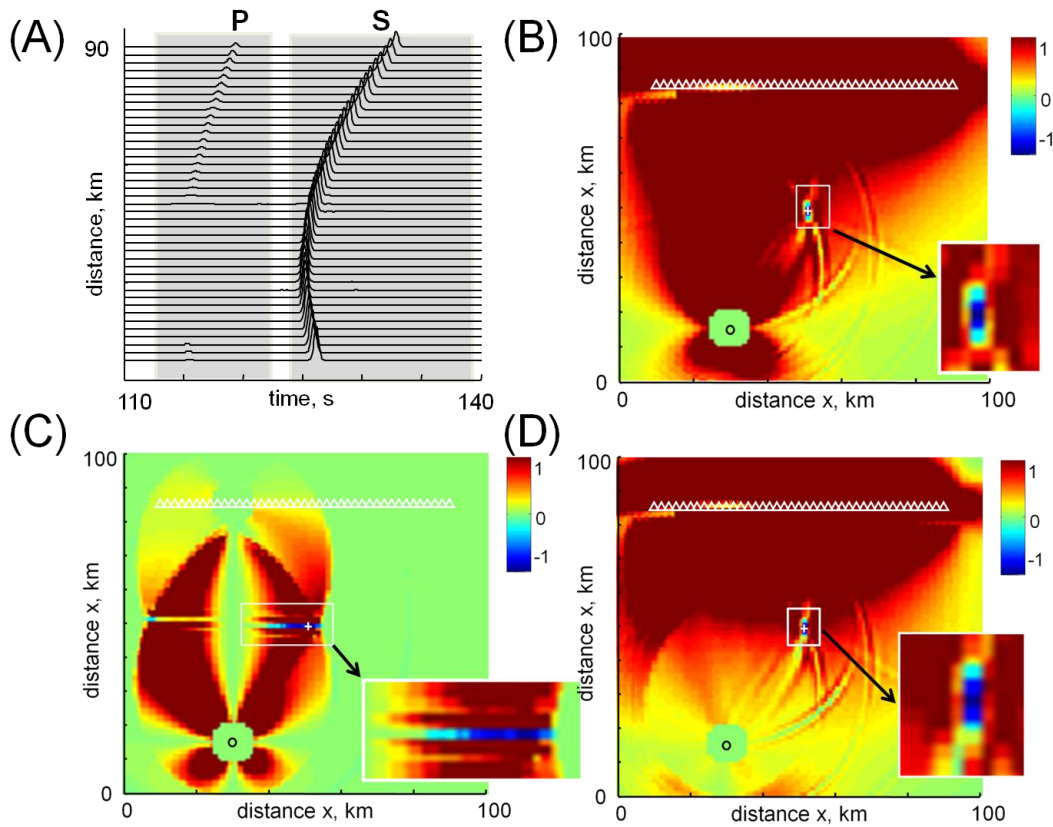
1120 Fig. 4. Geometry used in the cross-convolution example See text for further discussion.

1121



1123

1124 Fig. 5. Quantities associated with the cross-convolution partial derivative $\partial\Psi/\partial m$ and the power
 1125 partial derivative $\partial P/\partial m$. (A) The window function Ω . (B) The horizontal (black) and vertical
 1126 (red) components of the unperturbed field at the observer. (C) The horizontal (black) and vertical
 1127 (red) components of the observed field at the observer, after windowing. (D) The four
 1128 components of the cross-correlation function \mathbf{X} . (E) The source $\boldsymbol{\varphi}$ of the adjoint field $\boldsymbol{\lambda}$ (F) The
 1129 second derivative of the unperturbed field at a heterogeneity (location marked on Part I). (G) The
 1130 adjoint field $\boldsymbol{\lambda}$, which is associated with the cross-correlation measure. (H) The adjoint field $\boldsymbol{\xi}$,
 1131 which is associated with power. (I) The partial derivative $\partial\Psi/\partial m$ (colors) for point density
 1132 homogeneities distributed on the (x, y) plane. The source and receiver and the heterogeneity
 1133 singled out in Parts A-H are shown (circles) and the contribution of various scattering
 1134 interactions are made. (J) Same as Part I, but for the partial derivative $\partial P/\partial m$. (K) Same as Part
 1135 I, but for the partial derivative $\partial\Phi/\partial m$.

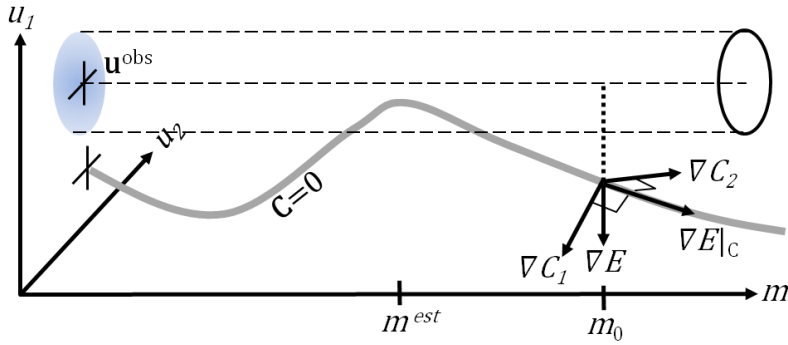


1137

1138 Fig.6. Quantities associated with the resolution test of the cross-convolution method. (A) The
 1139 horizontal-component of the wave field (curves) is observed by a linear array of receivers and is
 1140 due to a source in an elastic medium containing a “true” point heterogeneity (located in the white
 1141 box in Part B).. The vertical component (not shown) was also used. P and S wave windows are
 1142 shown (gray shading). (B) The partial derivative $\partial\Phi/\partial m$ (colors) for point density
 1143 homogeneities distributed on the (x, y) plane. The source (circle) is at the lower left and the
 1144 linear array of receivers (line of triangles) is near the top. The minimum (inset, blue) is
 1145 collocated with the true heterogeneity and is spatially-localized, implying excellent resolution.
 1146 (C) Same as Part B, except that the data are windowed around the P wave arrival. (C) Same as
 1147 Part B, except windowed around for the S wave.

1148

1149 Menke, Figure 7 (really Figure A.1.)



1150

1151 Fig. A.1. Geometrical interpretation of the process of computing the gradient of the total error

1152 subject to constraints that the field satisfies a differential equation. See text for further

1153 discussion.

1154

1155